

1 The authors like to thank Referee#1 for his comments and suggestions. The Referee's
2 comments and questions are bold, the authors' replies are formatted as plain text, and excerpts
3 from the manuscript as well as changes to the manuscript are given in italics.

4 **Reply to Anonymous Referee #1**

5 **While CO₂ is the most important greenhouse gas, its sources and sinks are still not well**
6 **understood. Studies of the carbon cycle require qualitatively good and long-term**
7 **measurements. Beside in-situ observations remote sensing observations have become an**
8 **important tool to study the carbon cycle. This paper forms an important contribution**
9 **for such studies. While so far most remote sensing observations are performed in the**
10 **near-infrared spectral region, organize in TCCON, this paper presents observations in**
11 **the mid-infrared, organized in the NDACC. Since most NDACC observations cover a**
12 **longer-time span, it makes sense to perform such studies also in the mid-infrared. This**
13 **holds especially for the Jungfrauoch site, where, together with the Kitt-Peak studies in**
14 **the US, the longest mid-infrared observations exist. The long-term data set presented,**
15 **and especially the studies of the seasonality together with the footprint analysis are**
16 **important and new scientific contributions.**

17 **The paper is well written and I have only a few comments.**

18 **Major comments:**

19 **The results of the paper depend on the comparability of near-infrared with mid-infrared**
20 **observations. This needs to be studied in much more detail. Great care has to be taken in**
21 **order to consider the different sensitivities of both infrared techniques to understand**
22 **differences and potential biases.**

23 The goal of this study is to compare in-situ measurements of a NonDispersive InfraRed
24 analyzer (NDIR) with column measurements from a Fourier Transform InfraRed (FTIR, mid
25 infrared) system, and to find out whether their different samples (surface air vs. column above
26 the station) provide similar results for the annual CO₂ change, the seasonality or even shorter-
27 lived CO₂ signals, or not. The physical characteristics of the CO₂ adsorption of both methods
28 is not subject of the present study and would be beyond the scope of this publication.

29 **Recently two papers have been published where these differences are studied in detail.**
30 **Barthlott et al, AMT, 2015 and Buschmann et al., AMT, 2016. The authors mention**
31 **shortly the paper by Barthlott, but do not mention the paper by Buschmann et al.**

32 Buschman et al., (2016) was added to the references and page 9, line 7 was changed from:

33 *“With a Monte Carlo algorithm, the values of the annual change of the CO₂ mole fraction of*
34 *the two datasets were calculated. Despite the shift between the two datasets of roughly 13*
35 *ppm (i.e. about 3%, in line with the systematic uncertainty affecting the FTIR measurement;*
36 *see section 2.3) and the different measurement techniques the annual CO₂ increase is quite*
37 *similar. The FTIR slope is 2.04 ± 0.07 ppm yr⁻¹ and the NDIR dataset shows a slope of $1.97 \pm$*
38 *0.05 ppm yr⁻¹, so they are equal within their uncertainties (Figure 4).”*

39 to:

1 “With a Monte Carlo algorithm, the values of the annual change of the CO₂ mole fraction of
2 the two datasets were calculated. Despite the shift between the two datasets of roughly 13
3 ppm and the different measurement techniques the annual CO₂ increase is quite similar. The
4 FTIR slope is 2.04 ± 0.07 ppm yr⁻¹ and the NDIR dataset shows a slope of 1.97 ± 0.05 ppm yr⁻¹,
5 so they are equal within their uncertainties (Figure 4). The observed offset between the
6 FTIR (NDACC) and in-situ records at Jungfraujoch contrasts the comparison of NDACC and
7 TCCON records as determined at Ny-Ålesund which do not show any offset at all when using
8 several individual CO₂ lines for the mid-IR (Buschmann et al., 2016). However, the
9 FTIR/NDIR offset of about 3% is commensurate with the systematic uncertainty affecting the
10 FTIR measurement; see section 2.3.”

11 **Since the study of the comparability of the mid-infrared data set from Jungfraujoch**
12 **with near-infrared observations, as performed within TCCON, are extremely**
13 **important, the results should be discussed and interpreted with respect to both papers.**

14 Unfortunately, there are no TCCON measurements at Jungfraujoch to compare with.

15 **Besides the presentation of the CO₂-data, section 2.3 of the manuscript form the most**
16 **important part of the paper, and much more details on the analysis should be given.**

17 In our opinion, the two measurement systems are equally important. Both measurement
18 systems provide an independent, valuable data set, which we compared.

19 We added some more detail to the section 2.3. It was changed at page 5, line 3 from:

20 “The uncertainty on the main CO₂ line strength is estimated at 2 to less than 5% in the
21 HITRAN compilation (Rothman et al., 2005), leading to a systematic error on the retrieved
22 total column of the same magnitude. In the meantime, the data set has been consistently
23 updated, still using the SFIT-1 algorithm (version 1.09c) and a single microwindow spanning
24 the 2024.3 – 2024.7 cm⁻¹ spectral interval, whose main spectral line is coming from ¹³CO₂.
25 The single CO₂ a priori vertical distribution used in all retrievals is characterized by a
26 constant mixing ratio of 338 ppm from the surface up to the tropopause, then slightly
27 decreasing to stabilize at 330 ppm at 20 km and above. A simple scaling retrieval is
28 performed, and the mixing ratio derived for the troposphere is used in the present
29 comparisons. Note that the representativeness of this unique profile is not optimal for all
30 seasons and may lead to an underestimation of the seasonal amplitude (see Fig. 1 in Barthlott
31 et al., 2015), because of a non-optimum vertical sensitivity of the FTIR retrieval. Indeed,
32 typical values of the total column averaging kernel – indicative of the fraction of information
33 coming from retrieval rather than from the a priori (e.g. Vigouroux et al., 2015) – are in the
34 0.5 – 1 range between the ground and 10 km altitude, in line with Fig. 4 of Barthlott et al.
35 (2015).”

36 to:

37 “In the meantime, the data set has been consistently updated, still using the SFIT-1 algorithm
38 (version 1.09c) and a single microwindow spanning the 2024.3 – 2024.7 cm⁻¹ spectral
39 interval, whose main spectral line at 2024.564 cm⁻¹ is coming from ¹³CO₂. The uncertainty
40 range on the strength of this CO₂ line is estimated at 2 to less than 5 % in the HITRAN
41 compilation (Rothman et al., 2005), leading to a systematic error on the retrieved total

1 column of the same magnitude. The single CO₂ a priori vertical distribution used in all
2 retrievals is characterized by a constant mixing ratio of 338 ppm from the surface up to the
3 tropopause, then slightly decreasing to stabilize at 330 ppm at 20 km and above. During the
4 retrieval process, a simple scaling of the whole vertical profile is performed, accounting for
5 interferences by weak ozone and water vapor lines, and the mixing ratio derived for CO₂ in
6 the troposphere is used in the present comparisons. Note that the representativeness of this
7 unique profile is not optimal for all seasons and may lead to an underestimation of the
8 seasonal amplitude (see Fig. 1 in Barthlott et al., 2015), because of a non-optimum vertical
9 sensitivity of the FTIR retrieval. Indeed, typical values of the total column averaging kernel –
10 indicative of the fraction of information coming from retrieval rather than from the a priori
11 (e.g. Vigouroux et al., 2015) – are in the 0.5 – 1 range between the ground and 10 km
12 altitude, in line with Fig. 4 of Barthlott et al. (2015). Over all the standard deviation of
13 multiple measurements over the course of a single day corresponds to less than one ppm,
14 which is significantly smaller than the observed seasonal cycle.”

15 **Minor comments:**

16 **The introduction is quite interesting and detailed, but very long. To me, many details**
17 **about the carbon cycle are not worth mentioning here, this part should be shortened.**

18 The part about the carbon cycle in the introduction was shortened, it reads now from page 2,
19 line 16 to page 3, line 4:

20 “CO₂ is the most important anthropogenic greenhouse gas, with a large contribution to the
21 greenhouse effect (Arrhenius, 1896) and an additional radiative forcing of the atmosphere
22 currently evaluated at 1.68 Wm⁻² (IPCC, 2013). The strength of the forcing is depending on
23 its atmospheric mole fraction which is ruled by the processes of the carbon cycle as well as by
24 anthropogenic CO₂ emissions from fossil fuel combustion and land use change. The major
25 reservoirs of the carbon cycle besides the lithosphere are the soils, the ocean, the biosphere
26 and the atmosphere, where the latter is also acting as the main link between the biosphere
27 and the ocean. The linking process between the atmosphere and the ocean is dissolution of
28 CO₂ in oceanic water, where it is subsequently chemically bound to bicarbonate and
29 carbonate and therefore removed from the carbon cycle on a longer timescale (Broecker and
30 Peng, 1982; Feely et al., 2004; Heinze et al., 1991; Sillén, 1966). The processes coupling the
31 biosphere with the atmosphere are photosynthesis, where CO₂ is taken up by plants, and
32 respiration, where CO₂ is released back to the atmosphere. Photosynthesis and respiration
33 are mainly driven by climatic conditions of the environment. In the northern hemisphere,
34 especially in the extratropics with distinct seasons, the dominating process in late spring,
35 summer and fall is photosynthesis and thereby the uptake of CO₂ from the atmosphere. In
36 autumn respiration and with it the release of CO₂ from the biosphere into the atmosphere
37 starts to take over and is the ruling process in winter until spring when photosynthesis
38 becomes the dominating process again. Due to these alternating processes, the CO₂ mole
39 fraction in the atmosphere shows a seasonal cycle with its maximum generally in early spring
40 and its minimum in fall (Halloran, 2012; Keeling et al., 1976; Keeling et al., 2001; Machida et
41 al., 2002).”

42 **For me the Figures 10, 11 and 12 do not tell important new findings. I suggest skipping**
43 **these Figures, or showing only one instead.**

1 We disagree because if there were significant changes of the correlations with increasing time
2 shifts, increasing widths of the running mean or a combination of the two, these figures would
3 be extremely important because they would show it clearly. However, the lack of clear
4 changes in the correlation in combination with the sensitivity plots indicates that the short
5 term variability of the two signals can't be compared. Therefore we like to keep these figures.

6 **Page 7, line 1: The seasonality is also influenced by fossil fuel combustion, not only by**
7 **respiration and photosynthesis.**

8 We changed the sentence:

9 *“One is the linear increase due to fossil fuel combustion (trend) and one is the annual in- and*
10 *decrease due to respiration and photosynthesis (seasonality).”*

11 to:

12 *“One is the linear increase due to fossil fuel combustion (trend) and one is the annual in- and*
13 *decrease due to respiration and photosynthesis, and to a lesser degree due to fossil fuel*
14 *combustion (seasonality).”*

15 The authors like to thank Referee#2 for his comments and suggestions. The Referee's
16 comments and questions are bold, the authors' replies are formatted as plain text, and excerpts
17 from the manuscript as well as changes to the manuscript are given in italics.

18

19 **Reply to Anonymous Referee #2**

20 **Review of 'Intercomparison of in-situ NDIR and column FTIR measurements of CO₂ at**
21 **Jungfraujoch' by Schibig et al.**

22 **The paper by Schibig et al., shows a comparison of two very different measurement time**
23 **series at Jungfraujoch station in Switzerland. Ground-based as well as FTIR column**
24 **measurements from 2005-2013 are presented. The authors report a consistent trend for**
25 **both data sets which are in agreement with other stations on the northern hemisphere.**
26 **The FTIR data set is biased low by 13 ppmv since the stratospheric column reduces the**
27 **mean column value.**

28 We would have expected the FTIR dataset to be slightly lower, because of the lower CO₂
29 mole fraction in the stratosphere, but since the FTIR data set is biased high by 13 ppm, we
30 think this is caused by the uncertainty in the HITRAN compilation, which leads to a
31 systematic error on the retrieved total column values. Further, we expect the influence of the
32 stratosphere on the FTIR measurements to be significantly less than 13 ppm.

33 **The data are filtered for pollution events and clear sky conditions and evidence is**
34 **provided, that the variability of both data sets is partly due to local CO₂ variations. The**
35 **seasonality is shows very interesting differences between both data sets, which are not**
36 **explained fully. Both data sets show the seasonal minimum at the same time in August,**
37 **but different times for the maximum, which occurs in January for the FTIR data set and**

1 in March for the NDIR in-situ measurements. This is explained by different source
2 regions for the respective months on the basis of FLEXPART footprint calculations for
3 2009-2011. Differences in the vertical distribution are mentioned and particularly the
4 role of the CO₂ gradient at the tropopause is not really discussed. In general the
5 manuscript is well written and should be published in ACP, but the analysis of the
6 seasonal differences and the footprint analysis should be sharpened.

7 **Main comments:**

8 **The NDIR shows the minima in August as well as the FTIR, but the maxima show**
9 **differences in their time of occurrence. The FTIR shows the maximum for January**
10 **whereas the NDIR exhibits its maximum in March. I'm not sure if the FLEXPART**
11 **footprints in Figs. 6-8 do provide meaningful results for the free tropospheric partial**
12 **columns. I don't see for a long-lived tracer like CO₂ any reason why a ten day backward**
13 **footprint for the free troposphere should provide an indication of sources and sinks. For**
14 **the lowest layer this might be valid, but how does the respective footprint explain the**
15 **seasonal differences in the free troposphere?**

16 The vertical transport time scale in the troposphere is usually smaller than 10 days (as used in
17 our FLEXPART simulations). Therefore, the model particles are usually widely dispersed in
18 the troposphere after 10 days of transport. Although they won't be well mixing within the
19 whole northern hemispheric troposphere, the influence of surface source regions beyond the
20 10 day transport is usually sufficiently diluted and one does not find distinct signals from any
21 specific source region. This is also true for free tropospheric release (receptor) locations since
22 horizontal transport is faster in the troposphere and despite the absence of significant
23 turbulent dispersion the particle plumes disperse due to wind field divergences. Therefore, we
24 are convinced that the 10 day transport scale and derived surface residence times are
25 sufficient to allow a qualitative interpretation of the contribution from different potential
26 source areas.

27 **How different are the footprint distributions in January, March and August from the**
28 **other months? The different time of occurrence of the respective winter maxima is also**
29 **not explained by the footprints. Is it maybe caused by seasonality of e.g. warm conveyor**
30 **belts and therefore seasonality of the vertical tropospheric column? I suggest to analyze**
31 **the FLEXPART output for this.**

32 The footprints for the selected months are fairly representative for the respective season, with
33 the exception of the January footprints which revealed strong influence from northern Africa
34 at different vertical levels, which was not observed in other winter months. In order to further
35 analyze the influence on transport on the observed seasonal cycle, we analyzed the timing of
36 surface influence for different land regions and present this as a new figure and section in the
37 revised manuscript. This extended transport analysis is able to explain the observations in the
38 sense that we find an increased decoupling between the free troposphere and the land surface
39 north of 30°N during the winter months, whereas the influence from tropical land surfaces
40 south of 30°N was increased in winter. Both suggests lower CO₂ in the FT (free troposphere)
41 than at the surface and an interruption of the wintertime increase in the FT above JFJ due to
42 the onset of the decoupling and tropical influence just following the observed maximum in
43 February.”

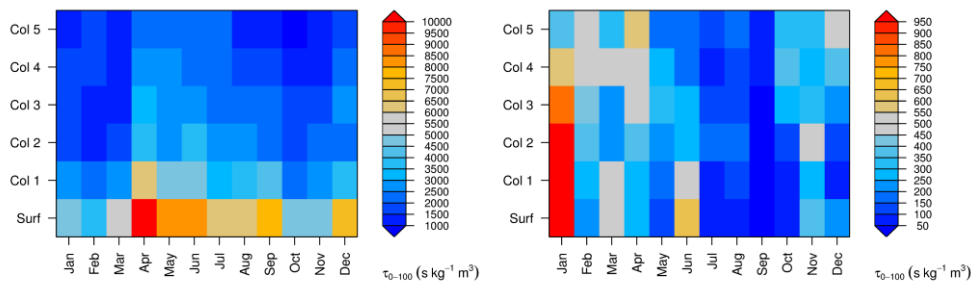
1 The following section was added at page 9, line 29:

2 “In general, the decoupling between the FTIR columns and possible surface fluxes of CO₂
3 from land surfaces north of 30°N was strongest during the winter month (January to March),
4 when especially low surface residence times were simulated by FLEXPART for the free
5 tropospheric FTIR columns (Figure 9). From April to September larger surface residence
6 times were seen also for the FTIR columns and a stronger coupling between surface fluxes
7 and the free troposphere can be expected. At the same time residence times over tropical land
8 surface (south of 30°N) were generally larger for the FTIR columns and were especially
9 increased from February to April (see Figure 9).

10 and page 13, line 6:

11 “...2009). The findings based on Figure 9 can help to understand the shift in the observed
12 wintertime maximum of CO₂ between FTIR (January) and NDIR (March-April) The land
13 surfaces of northern hemispheric mid-latitudes act as a net CO₂ source during the winter half
14 year, since photosynthesis is largely reduced and respiration and anthropogenic emissions of
15 CO₂ dominate the budget, hence, the observation of maximum CO₂ at the end of the winter
16 half year and close to the surface. For the free troposphere above JFJ as observed by the
17 FTIR the direct link to these wintertime releases of CO₂ is weakened due to generally reduced
18 vertical transport. At the same time more frequent transport from and land surface contact in
19 the tropics can be deduced, an area that even during the winter half year may act as a net
20 CO₂ sink due to photosynthetic uptake. An earlier onset of decreasing CO₂ in the FT above
21 Jungfraujoch could thereby be explained by different seasonality of transport and vertical
22 mixing. Additionally...”

23 And the following figure with caption was added as Figure 9:



24

25 Figure 9, Annual cycle of FLEXPART derived total surface residence time over land for
26 different vertical arrival columns above Jungfraujoch: (left) for land surfaces north of 30°N
27 and (right) for land surfaces south of 30°N.

28

29 Which role plays the seasonality of different tropopause height occurrence frequency
30 over JFJ in winter and summer for the interpretation of the CO₂ columns and the
31 summer - winter difference between FTIR and NDIR? Further as mentioned in the

1 **manuscript also the seasonality in the UTLS modifies the column. Is it possible to**
2 **quantify this a bit more?**

3

4 Indeed, this is an interesting, important, and valid point that hasn't been addressed in the
5 present work, therefore we cannot adequately reply to it. Generally, we would expect a lower
6 tropopause could potentially lower the column integrated CO₂ value due to the expected
7 lower stratospheric CO₂ mole fraction. A detailed analysis regarding this issue requires
8 substantial additional modeling, which was not possible within this work.

9 **p.5. l. 13: Please specify the long-term stability (i.e. error due to drift) and the total**
10 **uncertainty of the NDIR.**

11

12 The value given in the manuscript corresponds to the standard deviation of several cylinder
13 measurements each lasting at least one hour. The gas from the cylinders was treated,
14 calibrated, and evaluated exactly the same way as outside air, which is why we consider this
15 standard deviation as the precision of our system. The long term stability is taken care of by
16 frequent measurements of calibration gases (see section 2.2).

17 To make this clearer, we changed the sentence at page 5, line 14 from:

18

19 *“Cylinder measurements with a known mole fraction showed a precision better than 0.04 ppm*
20 *for 1 hour analysis.”*

21

22 to:

23

24 *“Cylinder measurements with a known mole fraction showed a long-term precision for hourly*
25 *averages better than 0.04 ppm. The accuracy of our target cylinder corresponds to less than*
26 *0.1 ppm (WMO target value for CO₂ measurements) calculated as standard deviation of the*
27 *mean considering the number of independent calibration set (high span, low span, working*
28 *gas).”*

29

30 **Technical: Fig.3: The caption refers to black lines or dots, which I can't find. Please**
31 **correct.**

32

33 That's correct, the caption refers to an older version of the figure. It was changed to:

34

35 *“Figure 3. A: Histogram of all NDIR residuals (yellow) and the filtered NDIR residuals*
36 *representing the background values (red) of the in-situ measurements; B: Histogram of all*
37 *FTIR residuals (light blue) and the filtered FTIR residuals representing the background*
38 *values (blue) of the column.”*

39

1 **Changes on the authors' behalf:**

2

3 The wavelength of the NDIR analyzer was added, p. 5, line 8 was changed from:

4

5 “...*NDIR spectrometer (Maihak S710) with a frequency ...*”

6

7 To:

8

9 “...*NDIR spectrometer (Maihak S710) measuring at a wavelength of 4.26 μm with a*
10 *frequency...*”

11

12 The Figures' numbers were updated because of the additional figure.

13

14 For more clarity, page 15, line 27 was changed from:

15 “...*or (c) since the FTIR retrievals has little vertical sensitivity the measured column signal*
16 *contains mixed information from the troposphere and the stratosphere.*”

17 to:

18 “...*or (c) since the FTIR vertical sensitivity was not exploited in the present retrievals the*
19 *measured column signal contains mixed information from the troposphere and the*
20 *stratosphere.*”

21

22 The reference of Rothman et al., (2005) at page 22, line 19 was moved down after Revelle et
23 al. (1957), to maintain the correct alphabetical order.

24

1 Intercomparison of in-situ NDIR and column FTIR 2 measurements of CO₂ at Jungfrauoch

3
4 **Michael F. Schibig¹, Emmanuel Mahieu², Stephan Henne³, Bernard Lejeune²,**
5 **Markus C. Leuenberger¹**

6 [1] Climate and Environmental Physics, Physics Institute and Oeschger Centre for Climate
7 Change Research, University of Bern, Bern, Switzerland

8 [2] Institut d'Astrophysique et de Géophysique, Université de Liège, Liège, Belgique

9 [3] Empa, Swiss Federal Laboratories for Materials Testing and Research, Dübendorf,
10 Switzerland

11 Correspondence to: leuenberger@climate.unibe.ch

12 Keywords: CO₂, FTIR, NDIR, Jungfrauoch, intercomparison, CO₂ trend

13 **Abstract**

14 We compare two CO₂ time series measured at the High Alpine Research Station Jungfrauoch
15 (3580 m a.s.l., Switzerland) in the period from 2005 to 2013 with an in-situ surface
16 measurement system using a nondispersive infrared analyzer (NDIR) and a ground-based
17 remote sensing system using solar absorption Fourier Transform Infrared spectrometry
18 (FTIR). Although the two data sets show an absolute shift of about 13 ppm, the slopes of the
19 annual CO₂ increase are in good agreement within their uncertainties. They are 2.04 ± 0.07
20 ppm yr^{-1} and $1.97 \pm 0.05 \text{ ppm yr}^{-1}$ for the FTIR and the NDIR system, respectively. The
21 seasonality of the FTIR and the NDIR system is $4.46 \pm 1.11 \text{ ppm}$ and $10.10 \pm 0.73 \text{ ppm}$,
22 respectively. The difference is caused by a dampening of the CO₂ signal with increasing
23 altitude due to mixing processes. While the minima of both data series occur in the middle of
24 August, the maxima of the two datasets differ by about ten weeks, the maximum of the FTIR
25 measurements is in middle of January, whereas the maximum of the NDIR measurements is
26 found at the end of March. Sensitivity analyses revealed that the air masses measured by the
27 NDIR system at the surface of Jungfrauoch are mainly influenced by central Europe, whereas
28 the air masses measured by the FTIR system in the column above Jungfrauoch are influenced
29 by regions as far west as the Caribbean and the United States.

1 The correlation between the hourly averaged CO₂ values of the NDIR system and the
2 individual FTIR CO₂ measurements is 0.820, which is very encouraging given the largely
3 different sampling volumes. Further correlation analyses showed, that the correlation is
4 mainly driven by the annual CO₂ increase and to a lesser degree by the seasonality. Both
5 systems are suitable to monitor the long-term CO₂ increase, because this signal is represented
6 in the whole atmosphere due to mixing.

7

8 **1 Introduction**

9 CO₂ is the most important anthropogenic greenhouse gas, with a large contribution to the
10 greenhouse effect (Arrhenius, 1896) and an additional radiative forcing of the atmosphere
11 currently evaluated at 1.68 Wm⁻² (IPCC, 2013). The strength of the forcing is depending on
12 its atmospheric mole fraction which is ruled by the processes of the carbon cycle as well as by
13 anthropogenic CO₂ emissions from fossil fuel combustion and land use change. The major
14 reservoirs of the carbon cycle besides the lithosphere are the soils, the ocean, the biosphere
15 and the atmosphere, where the latter is also acting as the main link between the biosphere and
16 the ocean. ~~The processes coupling the biosphere with the atmosphere are photosynthesis,~~
17 ~~where CO₂ is used by plants to convert solar energy into chemical energy by producing~~
18 ~~carbohydrates from CO₂ and H₂O, and respiration, the decomposition of biogenic~~
19 ~~carbohydrates back into CO₂, H₂O and energy, where CO₂ is released back to the atmosphere.~~
20 The linking process between the atmosphere and the ocean is dissolution of CO₂ in oceanic
21 water, where it is subsequently chemically bound to bicarbonate and carbonate and therefore
22 removed from the carbon cycle on a longer timescale (Broecker and Peng, 1982; Feely et al.,
23 2004; Heinze et al., 1991; Sillén, 1966). ~~The solution of CO₂ in water is depending on the~~
24 ~~partial pressures of CO₂ in the atmosphere and the ocean, if the atmospheric partial pressure~~
25 ~~of CO₂ above sea water is greater than the oceanic partial pressure of CO₂, CO₂ is taken up by~~
26 ~~the seawater and vice versa. Other factors as e.g. salinity, temperature etc. affect the solubility~~
27 ~~of CO₂ in seawater additionally (Bohr, 1899; Takahashi et al., 2009). The processes coupling~~
28 ~~the biosphere with the atmosphere are photosynthesis, where CO₂ is taken up by plants, and~~
29 ~~respiration, where CO₂ is released back to the atmosphere.~~ Photosynthesis and respiration, ~~on~~
30 ~~the other hand,~~ are mainly driven by climatic conditions of the environment. In the northern
31 hemisphere, especially in the extratropics with distinct seasons, the dominating process in late
32 spring, summer and fall is photosynthesis and thereby the uptake of CO₂ from the atmosphere.

1 In autumn respiration and with it the release of CO₂ from the biosphere into the atmosphere
2 starts to take over and is the ruling process in winter until spring when photosynthesis
3 becomes the dominating process again. Due to these alternating processes, the CO₂ mole
4 fraction in the atmosphere shows a seasonal cycle with its maximum generally in early spring
5 and its minimum in fall (Halloran, 2012;Keeling et al., 1976;Keeling et al., 2001;Machida et
6 al., 2002). A further component in the change of atmospheric CO₂ mole fraction is CO₂
7 release due to fossil fuel combustion (Karl and Trenberth, 2003;Revelle and Suess, 1957;Tans
8 et al., 1990). Nowadays, roughly half of the anthropogenically produced CO₂ ends up in the
9 oceans and the biosphere, whereas the other half is accumulating in the atmosphere and leads
10 to a more or less steady increase of the atmospheric CO₂ mole fraction (Bender et al., 2005;Le
11 Quéré et al., 2013;Sabine et al., 2004). Measuring the atmosphere's CO₂ mole fraction on the
12 long-term is therefore important to understand the sources and sinks of the carbon cycle and
13 the annual CO₂ increase due to fossil fuel combustion and land use change. To measure the
14 evolution of CO₂ in the atmosphere on a global scale satellite remote sensing methods can be
15 used as e.g. OCO-2 (Crisp et al., 2004, Pollock et al., 2010, Thompson et al., 2012) or
16 GOSAT (Chevallier et al., 2009, Yokota et al., 2009) but they are limited by e.g. cloud cover,
17 temporal coverage due to the orbit, coarse resolution etc. An intercomparison between
18 GOSAT and several TCCON (Total Carbon Column Observation Network) stations showed a
19 mean difference for daily averages of -0.34 ± 1.37 ppm (Heymann et al., 2015). Ground based
20 measurement systems on the other hand have a high temporal resolution and provide very
21 accurate data, which can be used to validate satellite data (Buchwitz et al., 2006; Butz et al.,
22 2011;Dils et al., 2006; Morino et al., 2011;Wunch et al., 2011) or as model input (Chevallier
23 et al., 2010), but surface observations have often a limited representativeness and are often
24 influenced by nearby processes and hence, not representative for larger areas. Also the
25 influence of the biosphere or anthropogenic pollution can be a serious issue and make it very
26 challenging to measure background air. Therefore, to measure global CO₂ trends the sampling
27 site should be at a very remote place like e.g. Mace Head Station (Bousquet et al.,
28 1996;Messenger et al., 2008) on the western coast of Ireland or the flask sampling network in
29 the Pacific of NOAA (Komhyr et al., 1985;Trolier et al., 1996). Another possibility is to
30 measure in the free troposphere e.g. with airplanes as done in the CARIBIC project
31 (Brenninkmeijer et al., 2007) or the CONTRAIL project (Machida et al., 2008) or at high
32 altitudes which are mostly in the free troposphere as e.g. Mauna Loa (Keeling et al.,
33 1976;Keeling et al., 1995;Pales and Keeling, 1965;Thoning et al., 1989). The High Alpine

1 Research Station Jungfraujoch (JFJ) with its altitude of 3580 m a.s.l. (Sphinx Observatory)
2 and position mostly above the planetary boundary (Henne et al., 2010) is therefore a very
3 suitable spot to conduct ground based CO₂ background measurements.

4 The University of Liège (Belgium) has been measuring infrared radiation at JFJ since the
5 1950s and started regular FTIR (Fourier Transform InfraRed) measurements in 1984. The
6 Climate and Environmental Physics Division (KUP) of the University of Bern started
7 measuring CO₂ and δO₂/N₂ in 2000 by a flask sampling program and since the end of 2004,
8 CO₂ and O₂ have been additionally measured with a continuously operating system of a NDIR
9 instrument and a paramagnetic cell. In this study we compared the FTIR and the NDIR data
10 set to see if the two complementary measurement techniques are catching the same trends,
11 seasonalities and variations in atmospheric CO₂ mole fraction at and above Jungfraujoch.

12

13 **2 Methods**

14 **2.1 Measurement site**

15 The High Altitude Research Station Jungfraujoch (JFJ) is located 7°59'02'' E, 46°32'53'' N
16 at the northern margin of the Swiss Alps. The Jungfraujoch is a mountain saddle between the
17 Mönch (4099 m a.s.l.) and Jungfrau (4158 m a.s.l.) summits at a height of 3580 m a.s.l.
18 (Sphinx Observatory) and is accessible year-round by train. Because of the high elevation, the
19 station is usually above the planetary boundary layer (PBL) and therefore mainly receives air
20 from the free troposphere which is why it was classified as “mostly remote” by Henne et al.
21 (2010). Nevertheless, the station can be influenced by polluted air during specific events such
22 as frontal passages and Föhn (Uglietti et al., 2011; Zellweger et al., 2003) or thermal uplift of
23 polluted air from the surrounding valleys on fair weather days (Baltensperger et al., 1997;
24 Henne et al., 2005; Zellweger et al., 2000). Because of the high elevation, the accessibility and
25 the good infrastructure, the JFJ is an ideal location for in-situ measurements of atmospheric
26 background air from continental Europe (Baltensperger et al., 1997; Henne et al.,
27 2010; Zellweger et al., 2003). JFJ is also one of the currently 29 core sites of the WMO GAW
28 (Global Atmospheric Watch) programme.

1 2.2 In-situ NDIR measurements at Jungfraujoch

2 The KUP CO₂ measurements are based on a combined system to monitor CO₂ and O₂
3 changes in the atmosphere. The ambient air is entering through a strongly ventilated (600
4 m³ h⁻¹) common inlet on the observatory's roof to a manifold, which serves many trace gas
5 analyzers, where an aliquot of it is drawn to the KUP system. The air is cryogenically dried to
6 a dew point of -90 °C (FC-100D21, FTS systems, USA). Temperature as well as pressure is
7 stabilized to avoid influences caused by ambient air density fluctuations. This allows the
8 determination of CO₂ by a NDIR spectrometer (Maihak S710) measuring at a wavelength of
9 4.26 μm with a frequency of 1 Hz and O₂ by a paramagnetic cell under highly controlled
10 conditions. Measurements are done in a cyclic sequence of 18 hours with each gas measured
11 for 6 minutes with only the last 115 seconds of a six minute period used for mole fraction
12 determination, to allow for signal stabilization after changing the sample source. At the
13 beginning of each 18-hour sequence, the system is calibrated with two reference gases (high
14 and low span). A working gas is measured between two ambient air measurements to correct
15 for short term variations. All measurements ending in a particular hour are used for the
16 calculation of hourly mean CO₂ observations, which in our case includes therefore 6 ambient
17 observation values per hour. Cylinder measurements with a known mole fraction showed a
18 long-term precision for hourly averages better than 0.04 ppm ~~for 1-hour analysis~~. The
19 accuracy of our target cylinder corresponds to less than 0.1 ppm (WMO target value for CO₂
20 measurements) calculated as standard deviation of the mean considering the number of
21 independent calibration set (high span, low span, working gas). The CO₂ values are reported
22 on the WMO X2007 scale. A multi-annual intercomparison between the NDIR system and a
23 cavity ring-down spectroscope at JFJ showed a very good agreement of the CO₂
24 measurements (Schibig et al., 2015).

Formatted: Subscript

25 2.3 Column FTIR measurements at Jungfraujoch

26 The University of Liège has been recording atmospheric solar spectra at JFJ since the early
27 1950s. The current FTIR instrument is a commercially available Bruker IFS-120 HR with a
28 resolution of up to 0.001 cm⁻¹ (Mahieu et al., 1997). It features interchangeable detectors, a
29 KBr beam-splitter and dedicated optical filters, which altogether give the possibility to cover
30 the 1 to 14 μm spectral range (Zander et al., 2008). Here gases such as CO₂, CH₄ and H₂O
31 show numerous absorption lines documenting contributions to the greenhouse effect. These

1 spectra also contain information about the abundance of many additional absorbing gas
2 species in the path between the instrument and the sun, essentially present either in the
3 troposphere or in the stratosphere. The CO₂ data set used here has been derived from the
4 reference total column time series produced within the framework of the NDACC monitoring
5 program (Network for the Detection of Atmospheric Composition Change; see
6 <http://www.ndacc.org>), presented previously in e.g. Zander et al. (2008; see Figure 6). ~~The
7 uncertainty on the main CO₂ line strength is estimated at 2 to less than 5% in the HITRAN
8 compilation (Rothman et al., 2005), leading to a systematic error on the retrieved total column
9 of the same magnitude.~~ In the meantime, the data set has been consistently updated, still
10 using the SFIT-1 algorithm (version 1.09c) and a single microwindow spanning the 2024.3 –
11 2024.7 cm⁻¹ spectral interval, whose main spectral line at 2024.564 cm⁻¹ is coming from
12 ¹³CO₂. The uncertainty range on the strength of this CO₂ line is estimated at 2 to less than 5 %
13 in the HITRAN compilation (Rothman et al., 2005), leading to a systematic error on the
14 retrieved total column of the same magnitude. The single CO₂ a priori vertical distribution
15 used in all retrievals is characterized by a constant mixing ratio of 338 ppm from the surface
16 up to the tropopause, then slightly decreasing to stabilize at 330 ppm at 20 km and above.
17 During the retrieval process, A simple scaling ~~retrieval of the whole vertical profile~~ is
18 performed, accounting for interferences by weak ozone and water vapor lines, and the mixing
19 ratio derived for CO₂ in the troposphere is used in the present comparisons. Note that the
20 representativeness of this unique profile is not optimal for all seasons and may lead to an
21 underestimation of the seasonal amplitude (see Fig. 1 in Barthlott et al., 2015), because of a
22 non-optimum vertical sensitivity of the FTIR retrieval. Indeed, typical values of the total
23 column averaging kernel – indicative of the fraction of information coming from retrieval
24 rather than from the a priori (e.g. Vigouroux et al., 2015) – are in the 0.5 – 1 range between
25 the ground and 10 km altitude, in line with Fig. 4 of Barthlott et al. (2015). Over all the
26 standard deviation of multiple measurements over the course of a single day corresponds to
27 less than one ppm, which is significantly smaller than the observed seasonal cycle.

Formatted: Superscript

Formatted: Subscript

Formatted: Subscript

28 2.4 Data processing

29 The NDIR data set is much more influenced by near ground processes like thermal uplift of
30 PBL air from the surrounding valleys, advection of PBL air by synoptic events etc. than the
31 FTIR and shows therefore a higher variability. Additionally, because of the large volume of
32 the column sampled by the FTIR above JFJ the CO₂ mole fraction measured by the FTIR is

1 averaged and the data set is far less sensitive to local events than the in-situ NDIR
2 measurements. The FTIR needs a cloudless sky to be able to measure, whereas the NDIR
3 system is measuring under all conditions, which can lead to very high CO₂ mole fractions
4 during e.g. Föhn events, when the sky is cloudy and polluted air from the heavily
5 industrialized Po basin (Northern Italy) is advected to JFJ. Therefore, only measurements of
6 background air should be taken into account to compare the two data sets properly.

7 **2.4.1 Filtering, trend and seasonality calculation**

8 The background data were selected using a statistical approach. A cubic spline was fitted to
9 both datasets individually, the standard deviation of the residuals was calculated and all points
10 beyond 2.7 σ were flagged as outliers. This process was repeated in both data sets until
11 convergence. The threshold of 2.7 σ was chosen because in normally distributed data more
12 than 99 % of the total data points would be included for further calculations and only the most
13 obvious outliers (less than 1 %) would be rejected.

14 The CO₂ mole fraction is dominated by two major processes. One is the linear increase due to
15 fossil fuel combustion (trend) and one is the annual in- and decrease due to respiration and
16 photosynthesis, and to a lesser degree due to fossil fuel combustion (seasonality). The trend
17 was calculated for both datasets individually with a Monte Carlo approach.

18 For the trend calculation we intentionally used the datasets including seasonal signals because
19 it leads to realistic trend error estimates compared to deseasonalized datasets, which in our
20 view tend to underestimate the error. The datasets were split in two subsets, where each of the
21 subsets spanned over $n - 0.5$ phases (in this study n equals 9 years) to prevent a bias in the
22 trend calculation due to the seasonal cycle. The first subsets start in January 2005, the second
23 subsets start in July 2005. In each subset about 2 % (a higher number does improve the result)
24 of the points were selected randomly and the linear trend was calculated. This was repeated
25 500 times with each subset and the averages of these linear trends were taken as the slopes of
26 the datasets.

27 To calculate the seasonality, the two datasets were detrended and monthly averages were
28 formed, from which the seasonality was calculated as the difference between the highest and
29 the lowest value.

1 **2.4.2 Correlation analysis**

2 Because of the different time resolutions for in-situ and FTIR measurements we selected
3 those in-situ measurements (six minute and hourly NDIR averages) that are closest (± 30 min)
4 to the FTIR values for correlation analysis.

5 Since the differences between both correlation analyses were negligible (see results section),
6 it was decided to continue with the hourly averages of the NDIR dataset only, which is the
7 common output of the NDIR database.

8 The FTIR's sample volume is much bigger than the NDIR system's and because of
9 transportation processes there's a possibility of mixing processes. To check, a moving average
10 of the NDIR data with increasing width was calculated to see if the correlation is enhanced
11 with expanding width (from 0 to ± 600 h).

12 Furthermore, the column measurements were retrieved for the layer between 3.58 km (altitude
13 of the Sphinx Observatory) to the top atmosphere (set to 100 km in the retrieval scheme)
14 whereas the NDIR system is measuring at the lower boundary of the FTIR's sampling
15 column, therefore it is possible that a time shift in the measured CO₂ mole fractions due to
16 advection, uplift of air parcels etc. occurs. To check whether a systematic time shift exists
17 between the two datasets, the NDIR measurements were shifted relative to the FTIR data
18 from -60 to +60 days (corresponding to -1440 h to +1440 h) in hourly steps and again the
19 correlation of the two data sets was calculated. If there is a systematic time shift, the deviation
20 should be indicated by increased correlation values.

21 **2.5 FLEXPART model runs**

22 From 2009 to 2011, backward Lagrangian particle dispersion model simulations were
23 performed with FLEXPART (Stohl, et al. 2005) to simulate the transport towards JFJ and
24 estimate surface source sensitivities (footprints) of the sampled air masses. To account for the
25 complex flow in the Alpine area, a regional scale version of the model driven by operational
26 output from the regional scale numerical weather prediction model COSMO as produced by
27 MeteoSwiss was used (Henne et al., 2015, Oney et al., 2015) . Since COSMO is a limited area
28 model, the transport of particles leaving the domain was further simulated in the global scale
29 version of FLEXPART (Stohl et al., 2005) driven by operational analysis fields of the
30 European Centre for Medium Range Weather Forecast (ECMWF). In the Alpine area,
31 COSMO input data had a horizontal resolution of approximately 2 km x 2 km, in Western
32 Europe 7 km x 7 km. Of the 1214 FTIR measurements in this period, footprints were

1 available for 766. The model simulated footprints of the surface in-situ observations and five
2 partial columns above JFJ reaching from 3365-4226 m a.s.l., 4226-4912 m a.s.l., 4912-5629
3 m a.s.l., 5629-6386 m a.s.l. and 6386-7184 m a.s.l. The lower boundary is below JFJ in order
4 to account for smoothed model topography. Particles released at and above JFJ were followed
5 10 days backward in time to calculate source sensitivities. Source sensitivities were evaluated
6 on regular longitude/latitude grids. The resolution was $0.5^\circ \times 0.5^\circ$ globally, $0.2^\circ \times 0.2^\circ$ over
7 Europe and an even higher resolution of $0.1^\circ \times 0.1^\circ$ was used in the Alpine area. The
8 footprints of the individual measurements of each partial column were averaged to monthly
9 means to get information about the origin of the air masses in the according month (Henne,
10 2014;Henne et al., 2013).

11

12 3 Results

13 Because of the different measurement techniques, the number of data points in the two
14 datasets is different. In the period 2005 to 2013 the NDIR dataset contains 68477 hourly
15 averages from which about 5 % were omitted as pollution or depletion events resulting from
16 PBL influence as estimated by the filtering (Figure 1). In the same period, the FTIR dataset
17 shows 3068 measurements of which about 5 % were rejected as pollution and depletion
18 events, too (Figure 2). For all further calculations, only the filtered datasets were used.

19 The average of the detrended and deseasonalized NDIR data before and after filtering was
20 0.00 ± 2.65 ppm and 0.00 ± 1.84 ppm (Figure 3 A), the average of the FTIR data was $0.01 \pm$
21 2.61 ppm and 0.01 ± 2.16 ppm, respectively (Figure 3 B).

22 With a Monte Carlo algorithm, the values of the annual change of the CO₂ mole fraction of
23 the two datasets were calculated. Despite the shift between the two datasets of roughly 13
24 ppm (~~i.e. about 3%, in line with the systematic uncertainty affecting the FTIR measurement;~~
25 ~~see section 2.3)~~ and the different measurement techniques the annual CO₂ increase is quite
26 similar. The FTIR slope is 2.04 ± 0.07 ppm yr⁻¹ and the NDIR dataset shows a slope of $1.97 \pm$
27 0.05 ppm yr⁻¹, so they are equal within their uncertainties (Figure 4). The observed offset
28 between the FTIR (NDACC) and in-situ records at Jungfraujoch contrasts the comparison of
29 NDACC and TCCON records as determined at Ny-Ålesund which do not show any offset at
30 all when using several individual CO₂ lines for the mid-IR, pointing to a calibration issue of
31 the FTIR measurements at Jungfraujoch in the order of their uncertainty (Buschmann et al.,

Formatted: Subscript

1 2016). However, the FTIR/NDIR offset of about 3% is commensurate in line with the range of
2 2% to 5% systematic uncertainty affecting the FTIR measurement; see section 2.3.

3 By detrending the datasets with the derived slopes, the seasonality can be calculated. The
4 column dataset shows a seasonality of 4.46 ± 1.11 ppm whereas the in-situ measurements at
5 the Sphinx Observatory show a seasonality roughly twice as big, namely 10.10 ± 0.73 ppm. To
6 find the moment of the average minima and maxima, a two harmonic fit function was applied
7 to the detrended datasets. The minima of the FTIR and NDIR datasets are both in the middle
8 of August, but the maxima are roughly ten weeks apart. The maximum of the NDIR datasets
9 occurs at the end of March, whereas seasonality of the FTIR dataset already reaches its
10 maximum in the middle of January (Figure 5).

11 The footprints of August, January and March, when the extrema of the seasonal cycle
12 occurred, as calculated with FLEXPART show that the in-situ observation at Jungfraujoch is
13 mainly receiving air masses that are influenced by Central Europe, and to a lesser degree by
14 the Mediterranean area and the northern Atlantic (Figure 6, Figure 7 and Figure 8).

15 With increasing altitude, the footprints of the sub-columns indicate, that the measured air
16 masses become more sensitive to regions as far west as e.g. the Caribbean and the United
17 States and that the influence from the European continent and northern regions higher than
18 50°N is decreasing (Figure 6, Figure 7 and Figure 8).

19 In general, the decoupling between the FTIR columns and possible surface fluxes of CO_2
20 from land surfaces north of 30°N was strongest during the winter month (January to March),
21 when especially low surface residence times were simulated by FLEXPART for the free
22 tropospheric FTIR columns (Figure 9). From April to September larger surface residence
23 times were seen also for the FTIR columns and a stronger coupling between surface fluxes
24 and the free troposphere can be expected. At the same time residence times over tropical land
25 surface (south of 30°N) were generally larger for the FTIR columns and were especially
26 increased from February to April (see Figure 9).

Formatted: English (U.S.)

Formatted: English (U.S.)

27 To estimate the relationship between the FTIR and NDIR measurements the correlation was
28 calculated. The FTIR measurements take normally about 10 min and are done whenever
29 possible. Therefore the FTIR data is reported exactly at the measuring time. The NDIR on the
30 other hand is measuring non-stop, but only 115 s of six-minute intervals (see methods) are
31 used to calculate a data point and the six-minute data is normally averaged to hourly averages.
32 Therefore we first checked whether the high resolution data are necessary or hourly data is
33 good enough. To do so, to each FTIR data point the nearest high resolution and hourly

1 averaged NDIR values were assigned. An additional condition was that the NDIR value must
2 not be further apart than ± 30 min, otherwise no NDIR data point was set, which was the case
3 in about 10 % of the FTIR data points. The correlation between the FTIR and the high
4 resolution NDIR CO₂ measurements and between the FTIR and the hourly averages were
5 calculated to be 0.819 and 0.820, so the differences between the two regression values are
6 negligible. To examine the relationship between the FTIR and the NDIR measurements
7 further, the seasonality of the two datasets was eliminated which gave almost the same
8 correlation of 0.824 (0.838 with the high resolution data). In the next step only the trend was
9 subtracted and the remaining seasonalities were compared, which lead to a much smaller
10 correlation of 0.460 (0.461 with the high resolution data). In a final step, the trend as well as
11 the seasonality was removed, which resulted in a correlation of 0.071 (0.084 high resolution
12 data vs. FTIR). Since correlations between the FTIR data and the NDIR's high resolution and
13 the hourly data were almost the same, only the hourly data was considered for further
14 calculations (Figure 10).

15 As mentioned above, the column measurements represent the whole vertical distribution
16 above Jungfraujoch whereas the NDIR system is measuring at the base of the FTIR's
17 sampling column. Therefore, the two records might be time-delayed due to advection, uplift
18 of air parcels etc. To check for a potential time lag, the NDIR measurements were shifted
19 relative to the FTIR data from -1440 to +1440 hours in hourly steps.

20 The correlations between the NDIR and FTIR datasets and between the deseasonalized NDIR
21 and FTIR datasets show a peak region at a time shift from -10 h to 60 h with the highest
22 correlation being 0.830 and 0.836 respectively (Figure 11 A, Figure 11 B). The correlation
23 between the datasets is decreasing before and after this range, in the deseasonalized datasets
24 the correlation stays more or less stable. The correlation between the two trend corrected
25 datasets shows a plateau of enhanced correlation values from -50 h to 200 h time shift with a
26 maximum correlation of 0.495 at a time shift of 165 h, at lower and higher time shifts, the
27 correlation is decreasing (Figure 11 C). The correlation of the detrended and deseasonalized
28 datasets shows no distinct pattern and is oscillating around 0 (Figure 11 D).

29 Since the air volume measured by the FTIR is much bigger than the NDIR system's volume,
30 vertical mixing and transport processes can occur and thereby changing the CO₂ mole fraction
31 in the measured air parcels. Therefore moving averages with increasing widths (up to ± 600 h)
32 were calculated from the NDIR data and the obtained averaged NDIR values were correlated
33 with the filtered FTIR dataset. Changing the width of the moving average doesn't have a

1 strong influence on the correlation between the two filtered datasets, because the increasing
2 width of the moving average just smooths the dataset. The correlation remains at about 0.85
3 (Figure 12 A), with a very small increase of the correlation at the beginning, most probably
4 due to the above mentioned smoothing effect. The same is true for the correlation between the
5 deseasonalized datasets. They show high correlation of about 0.84 over the whole range of
6 widths, with a slight increase at the beginning, which is not significant (Figure 12 B). By
7 detrending the datasets, the correlation is increasing with the width of the moving average and
8 shows a plateau of higher correlation of about 0.5 at a width 150 to 600 h from where on it is
9 decreasing again (Figure 12 C). However, the changes in the correlation within the range of
10 150 h to 600 h are very small. The detrended and deseasonalized datasets show a very low
11 correlation and the improvement of the correlation due to the changing width of the moving
12 average is negligible. Over all, the improvement of the correlations due to the changing width
13 of the moving average is very small (Figure 12 D).

14 Finally both, the time shift and the width of the moving average were varied about ± 1440 h
15 and ± 600 h, to see with which combination of time shift and width the best correlation can be
16 reached. They all show a ridge of higher correlation at a time shift around zero which is
17 broadening with increasing width of the moving average, except for the data without slope
18 and seasonality, which have a low correlation anyway (Figure 13). The increasing width of
19 the moving average leads to a small improvement of the correlations in the beginning,
20 however over all it doesn't seem to have a strong influence on the correlations. The time shift
21 on the other hand has an influence on correlation between the complete filtered datasets and
22 even more on the correlation of the detrended datasets. In the correlation of the
23 deseasonalized datasets, the influence of the time shift is very limited except for the small
24 ridge of slightly enhanced correlations around zero time shift as mentioned above.

25

26 **4 Discussion**

27 The filtered FTIR and NDIR datasets show a very similar increase in the CO₂ mole fraction of
28 ambient air, despite the two totally different measurement principles. The calculated annual
29 CO₂ trends of the FTIR and NDIR datasets are 2.04 ± 0.07 ppm yr⁻¹ and 1.97 ± 0.05 ppm yr⁻¹
30 respectively (Figure 4) and are in good agreement with flask measurements done at JFJ with a
31 slope of 1.85 ppm yr⁻¹ (van der Laan-Luijkx et al., 2013) and other remote stations in the
32 northern hemisphere; for example Mauna Loa with 2.05 ppm yr⁻¹ (Tans and Keeling, 2014) or

1 Alert with 1.85 ppm yr^{-1} (Keeling et al., 2001). Also the NDIR dataset's average seasonality
2 of $10.10 \pm 0.73 \text{ ppm}$ is in good agreement with the seasonality of these flask measurements,
3 which were $10.54 \pm 0.18 \text{ ppm}$ in the period 2007 to 2011 (van der Laan-Luijkx et al., 2013)
4 and is roughly double the FTIR's average seasonality of $4.46 \pm 1.11 \text{ ppm}$ (Figure 5). The
5 lower seasonality of the FTIR dataset can be explained by the fact that the NDIR system is
6 measuring CO_2 mole fractions at the Sphinx Observatory, which is most of the time above the
7 PBL (Henne et al., 2010) but still closer to the ground than the FTIR measurements.
8 Therefore the signal of the biosphere is stronger than in the column, where it is attenuated by
9 vertical mixing and transport processes of the atmosphere with increasing height. Also the
10 fixed a priori vertical CO_2 profile may contribute partly to the lower seasonality of the FTIR
11 measurements. The shape of the profile used to retrieve the CO_2 data doesn't reproduce the
12 changes due to seasonality and is therefore not always the optimum. By using a seasonally
13 varying a priori retrieval the seasonality might be slightly higher because the amplitude of
14 CO_2 is better retrieved (Barthlott et al., 2015). Furthermore, in the tropopause and the lower
15 stratosphere, the phase of the CO_2 seasonality is shifted by several months (Bönisch et al.,
16 2008; Gurk et al., 2008; Bönisch et al., 2009). However, this has only a minor influence on the
17 observed dampening of the amplitude of the FTIR seasonality compared to the vertical
18 mixing, since the stratosphere contains only about 10 % of the abundance of atmospheric air
19 molecules.

20 It is not easy to define the seasonal minimum and maximum in the FTIR dataset because they
21 are not very clearly pronounced. By fitting a two harmonic function the minimum was found
22 to be in the middle of August, the maximum in the middle of January. While the minimum of
23 the NDIR dataset is around the same time, the maximum of the FTIR dataset occurs roughly
24 ten weeks earlier than the maxima of the NDIR dataset (Figure 5). The timing of the minima
25 of both datasets and the maximum of the NDIR dataset coincide quite well with net land-
26 atmosphere carbon flux changes from negative to positive values and vice versa (Zeng et al.,
27 2014). Therefore an alternative explanation is needed for the early maximum of the FTIR
28 dataset. Sensitivity analyses revealed that the upper tropospheric air originates from lower
29 latitudes than the in-situ air measured by the NDIR. Therefore the air measured by the FTIR
30 is partially decoupled from the increasing CO_2 values of the winter-time northern hemisphere.
31 Furthermore, the decoupling might be amplified by the weak overturn of tropospheric air in
32 winter. Towards spring, the tropospheric overturn speeds up again which results in
33 synchronous CO_2 minima for both datasets in August. Similar studies investigating CO at JFJ

1 also showed that JFJ is not only sensitive to Central Europe but also to regions as far west as
2 for example North America, the Pacific or even Asia and that the influence of these regions is
3 getting stronger with increasing height (Dils et al., 2011; Pfister et al., 2004; Zellweger et al.,
4 2009). The findings based on Figure 9 can help to understand the shift in the observed
5 wintertime maximum of CO₂ between FTIR (January) and NDIR (March-April). The land
6 surfaces of northern hemispheric midlatitudes act as a net CO₂ source during the winter half
7 year, since photosynthesis is largely reduced and respiration and anthropogenic emissions of
8 CO₂ dominate the budget, hence, the observation of maximum CO₂ at the end of the winter
9 half year and close to the surface. For the free troposphere above JFJ as observed by the FTIR
10 the direct link to these wintertime releases of CO₂ is weakened due to generally reduced
11 vertical transport. At the same time more frequent transport from and land surface contact in
12 the tropics can be deduced, an area that even during the winter half year may act as a net CO₂
13 sink due to photosynthetic uptake. An earlier onset of decreasing CO₂ in the free troposphere
14 above JFJ could thereby be explained by different seasonality of transport and vertical
15 mixing. Additionally, the assumption of a fixed a priori CO₂ vertical distribution to retrieve
16 the column integrated CO₂ concentration from the FTIR dataset may contribute partially to
17 the observed shift of ten weeks in the NDIR and FTIR maxima, because it is representing the
18 distribution in winter/spring inadequately.

19 Another hint that the two systems are not measuring the same air parcels can be found in
20 correlation analyses. After omitting outliers, which are mostly caused by synoptic events,
21 thermal uplift of polluted air from surrounding valleys, or other local to regional transport
22 events, the correlation of the two datasets is as large as 0.820, which is quite encouraging
23 considering the different nature of the measurements. By excluding the seasonality from both
24 datasets, the correlation stays almost the same, namely 0.824 but drops to 0.460 if the
25 seasonality is included but the annual CO₂ increase is subtracted. The comparison of the two
26 CO₂ datasets with the annual CO₂ increase and the seasonality subtracted showed a very low
27 correlation of 0.071, which is negligible (Figure 10 ~~Figure 9~~). Because of possible delays and
28 mixing effects of the CO₂ signal, the time shift as well as the width of the moving average
29 calculated on the hourly values of the NDIR CO₂ values was varied between ± 1440 h and up
30 to ± 600 h, respectively. Shifting the NDIR time relative to the FTIR measurement time
31 creates a ridge of higher correlations around 0 h time shift with a slight tendency towards
32 positive values (Figure 13 A). This ridge-like form is clearly pronounced in the correlation
33 plot between the complete filtered FTIR and NDIR datasets and even more in the datasets

1 without slope (Figure 13 C) than in the correlation of the datasets without seasonality (Figure
2 13 B). There it is very small and the correlation is high across the whole time shift and
3 averaging width. The constantly high correlation for deseasonalized datasets is due to both
4 datasets containing mostly background air whose CO₂ mole fraction changes are mainly
5 driven by the annual CO₂ increase and by the seasonality of the CO₂ signal. Since the larger
6 of the two, the seasonality, is subtracted the high correlation is mainly driven by the slope
7 which was calculated to be the same within uncertainties and stays more or less constant over
8 the examined period. Therefore, the time shift has almost no influence. The remaining
9 fluctuations in the CO₂ mole fractions with higher frequencies than the seasonality seem to
10 play a minor role, because they're almost not visible in the comparison of the datasets without
11 seasonality except for the small ridge (Figure 13 B), or there's no correlation at all, as in the
12 comparison of the two datasets without slope and seasonality (Figure 13 D). This is indicating
13 that the two measurement systems are not measuring the same air parcels, even not with a
14 certain delay, or that the CO₂ signal of the NDIR system which is measured at the lower end
15 of the FTIR column becomes diluted beyond recognition for FTIR by the air mixing
16 processes. The positive effect of the increasing width of the moving average on the
17 correlation is strongest, but still very low, around the first 100 h. Afterwards its main effect is
18 broadening the ridge of the slightly enhanced correlations. The reason for the broadening
19 effect of the increasing width is its smoothing effect on the NDIR values. With increasing
20 width, the influence of a specific NDIR point on the correlation becomes smaller and the
21 NDIR dataset evolves into a smooth sine like curve with decreasing amplitudes, similar to the
22 FTIR dataset, where this form is caused by the higher sampling volume and the dampening
23 due to mixing processes in the atmosphere. However, the small influence of the moving
24 average's width on the correlation means that the correlation of the in-situ and the column
25 measurement is mainly influenced by the slope and the seasonality. Short term fluctuations
26 play a minor role mainly because either their CO₂ signal is dampened too much to be seen in
27 the column measurement or it is not measured at all as e.g. diurnal cycles because of the
28 applied measurement methods.

29

30 **5 Conclusions**

31 Two datasets of CO₂ measurements at the High Altitude Research Station Jungfraujoch in the
32 period 2005 to 2013 were compared. The FTIR system is measuring the attenuation of solar

1 light at different wavelengths caused by molecules of light absorbing gas species in the
2 column between the Sphinx Observatory and the sun. From the obtained spectra, with the
3 knowledge of CO₂ specific extinction bands and the pressure distribution along the path of the
4 light, it is possible to calculate the CO₂ mole fraction in the column. The NDIR system is
5 measuring the CO₂ mole fraction of ambient air at the Sphinx Observatory which corresponds
6 to the lower boundary of the FTIR measurements. The two datasets were filtered with a
7 statistical approach to exclude CO₂ measurements which were influenced by recent transport
8 from the planetary boundary layer. The filtering caused a loss of about 5 % in both, the NDIR
9 and the FTIR dataset.

10 The annual CO₂ increase of the two datasets was calculated with a Monte Carlo approach.
11 Despite an average offset of 13 ppm between the two datasets, which is within the systematic
12 uncertainty affecting the FTIR measurement, the slopes were in good agreement, namely 2.04
13 ± 0.07 ppm yr⁻¹ in the FTIR measurements and 1.97 ± 0.05 ppm yr⁻¹ in the NDIR dataset. The
14 seasonality of the CO₂ signal of the NDIR and the FTIR system is 10.10 ± 0.73 ppm and 4.46
15 ± 1.11 ppm, respectively. The difference is caused by a dampening of the CO₂ signal with
16 increasing altitude due to mixing processes. While the minima of the two datasets both occur
17 in the simultaneously, the maxima of the FTIR dataset was found ten weeks earlier than the
18 NDIR maxima.

19 The difference in the occurrence of the minima is most probably caused by the different
20 transport history of the air masses measured at JFJ and in the column above JFJ. In January,
21 the in-situ system is measuring air from central Europe and the Mediterranean, whereas the
22 air masses of the column measurements are more affected by the subtropic Northern Atlantic.
23 With the onset of spring in Europe, the photosynthetic activity is increasing and the CO₂ mole
24 fraction of air measured by the in-situ system starts to decrease at the end of March. The two
25 filtered datasets as well as the two deseasonalized datasets show a high correlation, whereas
26 the correlation between the two detrended datasets is only mediocre and inexistent in the
27 between the two detrended and deseasonalized datasets. Neither shifting the time of the NDIR
28 measurements relative to the FTIR measurements nor increasing the width of the moving
29 average did increase the correlation between the two datasets significantly. The enhanced
30 correlation values around a time shift of zero indicates that (i) there isn't a systematic time
31 shift apparent and that (ii) the correlation between the two datasets is mainly driven by the
32 annual CO₂ increase and to a lesser degree by the seasonality. Therefore both measurement
33 systems are suitable to measure the annual CO₂ increase, because this signal is well mixed

1 within the atmosphere. Short term variations as the seasonality or daily variations are less or
2 not comparable, because (a) the transport history of the air parcels measured is different, (b)
3 the signal is mixed beyond recognition or (c) since the FTIR vertical sensitivity was not
4 exploited in the present retrievals ~~since the FTIR retrievals has little vertical sensitivity~~ the
5 measured column signal contains mixed information from the troposphere and the
6 stratosphere.

7

8 **Acknowledgements**

9

10 This work was financially supported by the Swiss National Science Foundation (SNF-Project
11 200020_134641) and the Federal Office of Meteorology and Climatology MeteoSwiss in the
12 framework of Swiss GCOS. We like to thank the International Foundation High Altitude
13 Research Stations Jungfrauoch and Gornergrat (HFSJG), especially the custodians Martin
14 Fischer, Felix Seiler and Urs Otz for changing the calibration gases cylinders of the NDIR
15 system and other maintenance work. Additionally the authors like to thank Hanspeter Moret
16 and Peter Nyfeler for his precious work and help in maintaining and repairing the systems in
17 the Laboratory in Bern and also at Jungfrauoch. The Belgian contribution to the present work
18 was mainly supported by the Belgian Science Policy Office (BELSPO) and the Fonds de la
19 Recherche Scientifique – FNRS, both in Brussels. FLEXPART simulations were carried out
20 in the framework of EC FP7 project NORS (grant agreement N° 284421). Additional support
21 was provided by MeteoSwiss (GAW-CH) and the Fédération Wallonie Bruxelles. We are
22 grateful to the many colleagues and collaborators who have contributed to FTIR data
23 acquisition.

24

1 **References**

- 2 Arrhenius, S.: XXXI. On the influence of carbonic acid in the air upon the temperature of the
3 ground, *Philosophical Magazine Series 5*, 41, 237-276, 10.1080/14786449608620846, 1896.
- 4 Baltensperger, U., Gäggeler, H. W., Jost, D. T., Lugauer, M., Schwikowski, M., Weingartner,
5 E., and Seibert, P.: Aerosol climatology at the high-alpine site Jungfraujoch, Switzerland,
6 *Journal of Geophysical Research: Atmospheres*, 102, 19707-19715, 10.1029/97JD00928,
7 1997.
- 8 Barthlott, S., Schneider, M., Hase, F., Wiegele, A., Christner, E., González, Y., Blumenstock,
9 T., Dohe, S., García, O. E., Sepúlveda, E., Strong, K., Mendonca, J., Weaver, D., Palm, M.,
10 Deutscher, N. M., Warneke, T., Notholt, J., Lejeune, B., Mahieu, E., Jones, N., Griffith, D.
11 W. T., Velasco, V. A., Smale, D., Robinson, J., Kivi, R., Heikkinen, P. and Raffalski, U.:
12 Using XCO₂ retrievals for assessing the long-term consistency of NDACC/FTIR data sets,
13 *Atmospheric Measurement Techniques*, 8(3), 1555–1573, doi:10.5194/amt-8-1555-2015,
14 2015.
- 15 Bender, M. L., Ho, D. T., Hendricks, M. B., Mika, R., Battle, M. O., Tans, P. P., Conway, T.
16 J., Sturtevant, B., and Cassar, N.: Atmospheric O₂/N₂ changes, 1993–2002: Implications for
17 the partitioning of fossil fuel CO₂ sequestration, *Global Biogeochemical Cycles*, 19, GB4017,
18 10.1029/2004GB002410, 2005.
- 19 ~~Bohr, C.: Definition und Methode zur Bestimmung der Invasions- und Evasionskoeffizienten
20 bei der Auflösung von Gasen in Flüssigkeiten. Werthe der genannten Constanten sowie der
21 Absorptionsefficienten der Kohlensäure bei Auflösung in Wasser und in
22 Chlornatriumlösungen, *Annalen der Physik Leipzig*, 62, 26, 1899.~~
- 23 Bönisch, H., Hoor, P., Gurk, C., Feng, W., Chipperfield, M., Engel, A., and Bregman, B.:
24 Model evaluation of CO₂ and SF₆ in the extratropical UT/LS region, *Journal of Geophysical
25 Research: Atmospheres*, 113, 10.1029/2007JD008829, 2008.
- 26 Bönisch, H., Engel, A., Curtius, J., Birner, T., and Hoor, P.: Quantifying transport into the
27 lowermost stratosphere using simultaneous in-situ measurements of SF₆ and CO₂, *Atmos.
28 Chem. Phys.*, 9, 5905-5919, 10.5194/acp-9-5905-2009, 2009.
- 29 Bousquet, P., Gaudry, A., Ciais, P., Kazan, V., Monfray, P., Simmonds, P. G., Jennings, S.
30 G., and O'Connor, T. C.: Atmospheric CO₂ concentration variations recorded at Mace Head,

1 Ireland, from 1992 to 1994, *Physics and Chemistry of the Earth*, 21, 477-481,
2 [http://dx.doi.org/10.1016/S0079-1946\(97\)81145-7](http://dx.doi.org/10.1016/S0079-1946(97)81145-7), 1996.

3 Brenninkmeijer, C. A. M., Crutzen, P., Boumard, F., Dauer, T., Dix, B., Ebinghaus, R.,
4 Filippi, D., Fischer, H., Franke, H., Frieß, U., Heintzenberg, J., Helleis, F., Hermann, M.,
5 Kock, H. H., Koeppel, C., Lelieveld, J., Leuenberger, M., Martinsson, B. G., Miemczyk, S.,
6 Moret, H. P., Nguyen, H. N., Nyfeler, P., Oram, D., O'Sullivan, D., Penkett, S., Platt, U.,
7 Pupek, M., Ramonet, M., Randa, B., Reichelt, M., Rhee, T. S., Rohwer, J., Rosenfeld, K.,
8 Scharffe, D., Schlager, H., Schumann, U., Slemr, F., Sprung, D., Stock, P., Thaler, R.,
9 Valentino, F., van Velthoven, P., Waibel, A., Wandel, A., Waschitschek, K., Wiedensohler,
10 A., Xueref-Remy, I., Zahn, A., Zech, U., and Ziereis, H.: Civil Aircraft for the regular
11 investigation of the atmosphere based on an instrumented container: The new CARIBIC
12 system, *Atmos. Chem. Phys.*, 7, 4953-4976, 10.5194/acp-7-4953-2007, 2007.

13 Broecker, W. S., and Peng, T.-H.: *Tracers in the Sea*, Lamont-Doherty Geological
14 Observatory, Palisades, New York, 1982.

15 Buchwitz, M., de Beek, R., Noël, S., Burrows, J. P., Bovensmann, H., Schneising, O.,
16 Khlystova, I., Bruns, M., Bremer, H., Bergamaschi, P., Körner, S., and Heimann, M.:
17 Atmospheric carbon gases retrieved from SCIAMACHY by WFM-DOAS: version 0.5 CO
18 and CH₄ and impact of calibration improvements on CO₂ retrieval, *Atmos. Chem. Phys.*, 6,
19 2727-2751, 10.5194/acp-6-2727-2006, 2006.

20 [Buschmann, M., Deutscher, N. M., Sherlock, V., Palm, M., Warneke, T., and Notholt, J.:](#)
21 [Retrieval of xCO₂ from ground-based mid-infrared \(NDACC\) solar absorption spectra and](#)
22 [comparison to TCCON, *Atmos. Meas. Tech.*, 9, 577-585, 10.5194/amt-9-577-2016, 2016.](#)

23 Butz, A., Guerlet, S., Hasekamp, O., Schepers, D., Galli, A., Aben, I., Frankenberg, C.,
24 Hartmann, J. M., Tran, H., Kuze, A., Keppel-Aleks, G., Toon, G., Wunch, D., Wennberg, P.,
25 Deutscher, N., Griffith, D., Macatangay, R., Messerschmidt, J., Notholt, J., and Warneke, T.:
26 Toward accurate CO₂ and CH₄ observations from GOSAT, *Geophysical Research Letters*, 38,
27 10.1029/2011GL047888, 2011.

28 Crisp, D., Atlas, R. M., Breon, F. M., Brown, L. R., Burrows, J. P., Ciais, P., Connor, B. J.,
29 Doney, S. C., Fung, I. Y., Jacob, D. J., Miller, C. E., O'Brien, D., Pawson, S., Randerson, J.
30 T., Rayner, P., Salawitch, R. J., Sander, S. P., Sen, B., Stephens, G. L., Tans, P. P., Toon, G.
31 C., Wennberg, P. O., Wofsy, S. C., Yung, Y. L., Kuang, Z., Chudasama, B., Sprague, G.,

1 Weiss, B., Pollock, R., Kenyon, D., and Schroll, S.: The Orbiting Carbon Observatory (OCO)
2 mission, *Advances in Space Research*, 34, 700-709,
3 <http://dx.doi.org/10.1016/j.asr.2003.08.062>, 2004.

4 Chevallier, F., Maksyutov, S., Bousquet, P., Bréon, F.-M., Saito, R., Yoshida, Y., and Yokota,
5 T.: On the accuracy of the CO₂ surface fluxes to be estimated from the GOSAT observations,
6 *Geophysical Research Letters*, 36, n/a-n/a, 10.1029/2009GL040108, 2009.

7 Chevallier, F., Ciais, P., Conway, T. J., Aalto, T., Anderson, B. E., Bousquet, P., Brunke, E.
8 G., Ciattaglia, L., Esaki, Y., Fröhlich, M., Gomez, A., Gomez-Pelaez, A. J., Haszpra, L.,
9 Krummel, P. B., Langenfelds, R. L., Leuenberger, M., Machida, T., Maignan, F., Matsueda,
10 H., Morguá, J. A., Mukai, H., Nakazawa, T., Peylin, P., Ramonet, M., Rivier, L., Sawa, Y.,
11 Schmidt, M., Steele, L. P., Vay, S. A., Vermeulen, A. T., Wofsy, S., and Worthy, D.: CO₂
12 surface fluxes at grid point scale estimated from a global 21 year reanalysis of atmospheric
13 measurements, *Journal of Geophysical Research: Atmospheres*, 115, D21307,
14 10.1029/2010JD013887, 2010.

15 Dils, B., De Mazière, M., Müller, J. F., Blumenstock, T., Buchwitz, M., de Beek, R.,
16 Demoulin, P., Duchatelet, P., Fast, H., Frankenberg, C., Gloudemans, A., Griffith, D., Jones,
17 N., Kerzenmacher, T., Kramer, I., Mahieu, E., Mellqvist, J., Mittermeier, R. L., Notholt, J.,
18 Rinsland, C. P., Schrijver, H., Smale, D., Strandberg, A., Straume, A. G., Stremme, W.,
19 Strong, K., Sussmann, R., Taylor, J., van den Broek, M., Velazco, V., Wagner, T., Warneke,
20 T., Wiacek, A., and Wood, S.: Comparisons between SCIAMACHY and ground-based FTIR
21 data for total columns of CO, CH₄, CO₂ and N₂O, *Atmos. Chem. Phys.*, 6, 1953-1976,
22 10.5194/acp-6-1953-2006, 2006.

23 Dils, B., Cui, J., Henne, S., Mahieu, E., Steinbacher, M., and De Mazière, M.: 1997–2007 CO
24 trend at the high Alpine site Jungfraujoch: a comparison between NDIR surface in situ and
25 FTIR remote sensing observations, *Atmos. Chem. Phys.*, 11, 6735-6748, 10.5194/acp-11-
26 6735-2011, 2011.

27 Feely, R. A., Sabine, C. L., Lee, K., Berelson, W., Kleypas, J., Fabry, V. J., and Millero, F. J.:
28 Impact of Anthropogenic CO₂ on the CaCO₃ System in the Oceans, *Science*, 305, 362-366,
29 10.1126/science.1097329, 2004.

1 Gurk, C., Fischer, H., Hoor, P., Lawrence, M. G., Lelieveld, J., and Wernli, H.: Airborne in-
2 situ measurements of vertical, seasonal and latitudinal distributions of carbon dioxide over
3 Europe, *Atmos. Chem. Phys.*, 8, 6395-6403, 10.5194/acp-8-6395-2008, 2008.

4 Halloran, P. R.: Does atmospheric CO₂ seasonality play an important role in governing the
5 air-sea flux of CO₂?, *Biogeosciences*, 9, 2311-2323, 10.5194/bg-9-2311-2012, 2012.

6 Heinze, C., Maier-Reimer, E., and Winn, K.: Glacial pCO₂ Reduction by the World Ocean:
7 Experiments With the Hamburg Carbon Cycle Model, *Paleoceanography*, 6, 395-430,
8 10.1029/91PA00489, 1991.

9 Henne, S., Furger, M., and Prévôt, A. S. H.: Climatology of Mountain Venting-Induced
10 Elevated Moisture Layers in the Lee of the Alps, *JOURNAL OF APPLIED*
11 *METEOROLOGY*, 44, 620-633, 10.1175/JAM2217.1, 2005.

12 Henne, S., Brunner, D., Folini, D., Solberg, S., Klausen, J., and Buchmann, B.: Assessment of
13 parameters describing representativeness of air quality in-situ measurement sites, *Atmos.*
14 *Chem. Phys.*, 10, 3561-3581, 10.5194/acp-10-3561-2010, 2010.

15 Henne, S., Steinbacher, M., Mahieu, E., Bader, W., Blumenstock, T., Cuevas-Agulló, E.,
16 Brunner, D., and Buchmann, B.: Comparison of ground-based remote sensing and in-situ
17 observations of CO, CH₄ and O₃ accounting for representativeness uncertainty, EGU General
18 Assembly, Vienna, Austria, 7-12 April 2013, 2013.

19 Henne, S., D. Brunner, B. Oney, M. Leuenberger, W. Eugster, I. Bamberger, F. Meinhardt,
20 M. Steinbacher, and L. Emmenegger, Validation of Swiss Methane Emission Inventory by
21 Atmospheric Observations and Inverse Modelling, *Atmos. Chem. Phys. Discuss.*, 15, 35417-
22 35484, doi: 10.5194/acpd-15-35417-2015, 2015.

23 Heymann, J., Reuter, M., Hilker, M., Buchwitz, M., Schneising, O., Bovensmann, H.,
24 Burrows, J. P., Kuze, A., Suto, H., Deutscher, N. M., Dubey, M. K., Griffith, D. W. T., Hase,
25 F., Kawakami, S., Kivi, R., Morino, I., Petri, C., Roehl, C., Schneider, M., Sherlock, V.,
26 Sussmann, R., Velasco, V. A., Warneke, T., and Wunch, D.: Consistent satellite XCO₂
27 retrievals from SCIAMACHY and GOSAT using the BESD algorithm, *Atmos. Meas. Tech.*,
28 8, 2961-2980, 10.5194/amt-8-2961-2015, 2015.

29 IPCC: Climate Change 2013: The Physical Science Basis. Contribution of Working Group I
30 to the Fifth Assessment Report of the Intergovernmental Panel on Climate Change,

1 Cambridge University Press, Cambridge, United Kingdom and New York, NY, USA, 1535
2 pp., 2013.

3 Karl, T. R., and Trenberth, K. E.: Modern Global Climate Change, *Science*, 302, 1719-1723,
4 10.1126/science.1090228, 2003.

5 Keeling, C. D., Bacastow, R. B., Bainbridge, A. E., Ekdahl, C. A., Guenther, P. R.,
6 Waterman, L. S., and Chin, J. F. S.: Atmospheric carbon dioxide variations at Mauna Loa
7 Observatory, Hawaii, *Tellus*, 28, 538-551, 10.1111/j.2153-3490.1976.tb00701.x, 1976.

8 Keeling, C. D., Whorf, T. P., Wahlen, M., and van der Plichtt, J.: Interannual extremes in the
9 rate of rise of atmospheric carbon dioxide since 1980, *Nature*, 375, 666-670, 1995.

10 Keeling, C. D., Piper, S. C., Bacastow, R. B., Wahlen, M., Whorf, T. P., Heimann, M., and
11 Meijer, H. A.: Exchanges of Atmospheric CO₂ and ¹³CO₂ with the Terrestrial Biosphere and
12 Oceans from 1978 to 2000. I. Global Aspects, SIO Reference Series, No. 01-06, Scripps
13 Institution of Oceanography, San Diego, 88, 2001.

14 Komhyr, W. D., Gammon, R. H., Harris, T. B., Waterman, L. S., Conway, T. J., Taylor, W.
15 R., and Thoning, K. W.: GLOBAL ATMOSPHERIC CO₂ DISTRIBUTION AND
16 VARIATIONS FROM 1968-1982 NOAA GMCC CO₂ FLASK SAMPLE DATA, *J.*
17 *Geophys. Res.-Atmos.*, 90, 5567-5596, 10.1029/JD090iD03p05567, 1985.

18 Le Quéré, C., Peters, G. P., Andres, R. J., Andrew, R. M., Boden, T., Ciais, P., Friedlingstein,
19 P., Houghton, R. A., Marland, G., Moriarty, R., Sitch, S., Tans, P., Armeth, A., Arvanitis, A.,
20 Bakker, D. C. E., Bopp, L., Canadell, J. G., Chini, L. P., Doney, S. C., Harper, A., Harris, I.,
21 House, J. I., Jain, A. K., Jones, S. D., Kato, E., Keeling, R. F., Klein Goldewijk, K.,
22 Körtzinger, A., Koven, C., Lefèvre, N., Omar, A., Ono, T., Park, G. H., Pfeil, B., Poulter, B.,
23 Raupach, M. R., Regnier, P., Rödenbeck, C., Saito, S., Schwinger, J., Segschneider, J.,
24 Stocker, B. D., Tilbrook, B., van Heuven, S., Viovy, N., Wanninkhof, R., Wiltshire, A.,
25 Zaehle, S., and Yue, C.: Global carbon budget 2013, *Earth Syst. Sci. Data Discuss.*, 6, 689-
26 760, 10.5194/essdd-6-689-2013, 2013.

27 Machida, T., Kita, K., Kondo, Y., Blake, D., Kawakami, S., Inoue, G., and Ogawa, T.:
28 Vertical and meridional distributions of the atmospheric CO₂ mixing ratio between northern
29 midlatitudes and southern subtropics, *Journal of Geophysical Research: Atmospheres*, 107,
30 8401, 10.1029/2001JD000910, 2002.

1 Machida, T., Matsueda, H., Sawa, Y., Nakagawa, Y., Hirotsu, K., Kondo, N., Goto, K.,
2 Nakazawa, T., Ishikawa, K., and Ogawa, T.: Worldwide Measurements of Atmospheric CO₂
3 and Other Trace Gas Species Using Commercial Airlines, *Journal of Atmospheric and*
4 *Oceanic Technology*, 25, 1744-1754, 10.1175/2008JTECHA1082.1, 2008.

5 Mahieu, E., Zander, R., Delbouille, L., Demoulin, P., Roland, G., and Servais, C.: Observed
6 Trends in Total Vertical Column Abundances of Atmospheric Gases from IR Solar Spectra
7 Recorded at the Jungfraujoch, *Journal of Atmospheric Chemistry*, 28, 227-243,
8 10.1023/A:1005854926740, 1997.

9 Messager, C., Schmidt, M., Ramonet, M., Bousquet, P., Simmonds, P., Manning, A., Kazan,
10 V., Spain, G., Jennings, S. G., and Ciais, P.: Ten years of CO₂, CH₄, CO and N₂O fluxes over
11 Western Europe inferred from atmospheric measurements at Mace Head, Ireland, *Atmos.*
12 *Chem. Phys. Discuss.*, 8, 1191-1237, 10.5194/acpd-8-1191-2008, 2008.

13 Morino, I., Uchino, O., Inoue, M., Yoshida, Y., Yokota, T., Wennberg, P. O., Toon, G. C.,
14 Wunch, D., Roehl, C. M., Notholt, J., Warneke, T., Messerschmidt, J., Griffith, D. W. T.,
15 Deutscher, N. M., Sherlock, V., Connor, B., Robinson, J., Sussmann, R., and Rettinger, M.:
16 Preliminary validation of column-averaged volume mixing ratios of carbon dioxide and
17 methane retrieved from GOSAT short-wavelength infrared spectra, *Atmos. Meas. Tech.*, 4,
18 1061-1076, 10.5194/amt-4-1061-2011, 2011.

19 Oney, B., Henne, S., Gruber, N., Leuenberger, M., Bamberger, I., Eugster, W., and Brunner,
20 D.: The CarboCount CH sites: characterization of a dense greenhouse gas observation
21 network, *Atmos. Chem. Phys. Discuss.*, 15, 12911-12956, 10.5194/acpd-15-12911-2015,
22 2015.

23 Pales, J. C., and Keeling, C. D.: The concentration of atmospheric carbon dioxide in Hawaii,
24 *Journal of Geophysical Research*, 70, 6053-6076, 10.1029/JZ070i024p06053, 1965.

25 Pfister, G., Pétron, G., Emmons, L. K., Gille, J. C., Edwards, D. P., Lamarque, J. F., Attie, J.
26 L., Granier, C., and Novelli, P. C.: Evaluation of CO simulations and the analysis of the CO
27 budget for Europe, *Journal of Geophysical Research: Atmospheres*, 109, D19304,
28 10.1029/2004JD004691, 2004.

29 Pollock, R., Haring, R. E., Holden, J. R., Johnson, D. L., Kapitanoff, A., Mohlman, D.,
30 Phillips, C., Randall, D., Rechsteiner, D., Rivera, J., Rodriguez, J. I., Schwochert, M. A., and

1 Sutin, B. M.: The Orbiting Carbon Observatory instrument: performance of the OCO
2 instrument and plans for the OCO-2 instrument, 2010, 78260W-78260W-78213, 2010.

3 ~~Rothman, L. S., Jacquemart, D., Barbe, A., Chris Benner, D., Birk, M., Brown, L. R., Carleer,~~
4 ~~M. R., Chackerian, C., Chance, K., Coudert, L. H., Dana, V., Devi, V. M., Flaud, J. M.,~~
5 ~~Gamache, R. R., Goldman, A., Hartmann, J. M., Jucks, K. W., Maki, A. G., Mandin, J. Y.,~~
6 ~~Massie, S. T., Orphal, J., Perrin, A., Rinsland, C. P., Smith, M. A. H., Tennyson, J.,~~
7 ~~Tolchenov, R. N., Toth, R. A., Vander Auwera, J., Varanasi, P. and Wagner, G.: The~~
8 ~~HITRAN 2004 molecular spectroscopic database, Journal of Quantitative Spectroscopy and~~
9 ~~Radiative Transfer, 96(2), 139–204, doi:10.1016/j.jqsrt.2004.10.008, 2005.~~

10 Revelle, R., and Suess, H. E.: Carbon Dioxide Exchange Between Atmosphere and Ocean and
11 the Question of an Increase of Atmospheric CO₂ during the Past Decades, Tellus, 9, 18-27,
12 10.1111/j.2153-3490.1957.tb01849.x, 1957.

13 ~~Rothman, L. S., Jacquemart, D., Barbe, A., Chris Benner, D., Birk, M., Brown, L. R., Carleer,~~
14 ~~M. R., Chackerian, C., Chance, K., Coudert, L. H., Dana, V., Devi, V. M., Flaud, J.-M.,~~
15 ~~Gamache, R. R., Goldman, A., Hartmann, J.-M., Jucks, K. W., Maki, A. G., Mandin, J.-Y.,~~
16 ~~Massie, S. T., Orphal, J., Perrin, A., Rinsland, C. P., Smith, M. A. H., Tennyson, J.,~~
17 ~~Tolchenov, R. N., Toth, R. A., Vander Auwera, J., Varanasi, P. and Wagner, G.: The~~
18 ~~HITRAN 2004 molecular spectroscopic database, Journal of Quantitative Spectroscopy and~~
19 ~~Radiative Transfer, 96(2), 139–204, doi:10.1016/j.jqsrt.2004.10.008, 2005.~~

20 Sabine, C. L., Feely, R. A., Gruber, N., Key, R. M., Lee, K., Bullister, J. L., Wanninkhof, R.,
21 Wong, C. S., Wallace, D. W. R., Tilbrook, B., Millero, F. J., Peng, T.-H., Kozyr, A., Ono, T.,
22 and Rios, A. F.: The Oceanic Sink for Anthropogenic CO₂, Science, 305, 367-371,
23 10.1126/science.1097403, 2004.

24 Sillén, L. G.: Regulation of O₂, N₂ and CO₂ in the atmosphere; thoughts of a laboratory
25 chemist, Tellus, 18, 198-206, 10.1111/j.2153-3490.1966.tb00226.x, 1966.

26 Stohl, A., Forster, C., Frank, A., Seibert, P., and Wotawa, G.: Technical note: The Lagrangian
27 particle dispersion model FLEXPART version 6.2, Atmos. Chem. Phys., 5, 2461-2474,
28 10.5194/acp-5-2461-2005, 2005.

29 ~~Takahashi, T., Sutherland, S. C., Wanninkhof, R., Sweeney, C., Feely, R. A., Chipman, D.~~
30 ~~W., Hales, B., Friederich, G., Chavez, F., Sabine, C., Watson, A., Bakker, D. C. E., Schuster,~~
31 ~~U., Metzl, N., Yoshikawa Inoue, H., Ishii, M., Midorikawa, T., Nojiri, Y., Körtzinger, A.,~~

1 ~~Steinhoff, T., Hoppema, M., Olafsson, J., Arnarson, T. S., Tilbrook, B., Johannessen, T.,~~
2 ~~Olsen, A., Bellerby, R., Wong, C. S., Delille, B., Bates, N. R., and de Baar, H. J. W.:~~
3 ~~Climatological mean and decadal change in surface ocean pCO₂, and net sea-air CO₂ flux~~
4 ~~over the global oceans, *Deep Sea Research Part II: Topical Studies in Oceanography*, 56, 554-~~
5 ~~577, <http://dx.doi.org/10.1016/j.dsr2.2008.12.009>, 2009.~~

6 NOAA Earth System Research Laboratory, Global Monitoring Division:
7 <http://www.esrl.noaa.gov/gmd/ccgg/trends/>, access: 30.10.2014, 2014.

8 Schibig, M. F., Steinbacher, M., Buchmann, B., van der Laan-Luijkx, I. T., van der Laan, S.,
9 Ranjan, S., and Leuenberger, M. C.: Comparison of continuous in situ CO₂ observations at
10 Jungfraujoch using two different measurement techniques, *Atmos. Meas. Tech.*, 8, 57-68,
11 10.5194/amt-8-57-2015, 2015.

12 Tans, P. P., Fung, I. Y., and Takahashi, T.: Observational Constrains on the Global
13 Atmospheric CO₂ Budget, *Science*, 247, 1431-1438, 10.1126/science.247.4949.1431, 1990.

14 Thompson, D. R., Chris Benner, D., Brown, L. R., Crisp, D., Malathy Devi, V., Jiang, Y.,
15 Natraj, V., Oyafuso, F., Sung, K., Wunch, D., Castaño, R., and Miller, C. E.: Atmospheric
16 validation of high accuracy CO₂ absorption coefficients for the OCO-2 mission, *Journal of*
17 *Quantitative Spectroscopy and Radiative Transfer*, 113, 2265-2276,
18 <http://dx.doi.org/10.1016/j.jqsrt.2012.05.021>, 2012.

19 Thoning, K. W., Tans, P. P., and Komhyr, W. D.: Atmospheric carbon dioxide at Mauna Loa
20 Observatory: 2. Analysis of the NOAA GMCC data, 1974–1985, *Journal of Geophysical*
21 *Research: Atmospheres*, 94, 8549-8565, 10.1029/JD094iD06p08549, 1989.

22 Trolier, M., White, J. W. C., Tans, P. P., Masarie, K. A., and Gemery, P. A.: Monitoring the
23 isotopic composition of atmospheric CO₂: Measurements from the NOAA Global Air
24 Sampling Network, *Journal of Geophysical Research: Atmospheres*, 101, 25897-25916,
25 10.1029/96JD02363, 1996.

26 Uglietti, C., Leuenberger, M., and Brunner, D.: European source and sink areas of CO₂
27 retrieved from Lagrangian transport model interpretation of combined O₂ and CO₂
28 measurements at the high alpine research station Jungfraujoch, *Atmos. Chem. Phys.*, 11,
29 8017-8036, 10.5194/acp-11-8017-2011, 2011.

30 van der Laan-Luijkx, I. T., van der Laan, S., Uglietti, C., Schibig, M. F., Neubert, R. E. M.,
31 Meijer, H. A. J., Brand, W. A., Jordan, A., Richter, J. M., Rothe, M., and Leuenberger, M. C.:

1 Atmospheric CO₂, δ(O₂/N₂) and δ¹³CO₂ measurements at Jungfraujoch, Switzerland: results
2 from a flask sampling intercomparison program, *Atmos. Meas. Tech.*, 6, 1805-1815,
3 10.5194/amt-6-1805-2013, 2013.

4 Vigouroux, C., Blumenstock, T., Coffey, M., Errera, Q., García, O., Jones, N. B., Hannigan,
5 J. W., Hase, F., Liley, B., Mahieu, E., Mellqvist, J., Notholt, J., Palm, M., Persson, G.,
6 Schneider, M., Servais, C., Smale, D., Thölix, L. and De Mazière, M.: Trends of ozone total
7 columns and vertical distribution from FTIR observations at eight NDACC stations around
8 the globe, *Atmospheric Chemistry and Physics*, 15(6), 2915–2933, doi:10.5194/acp-15-2915-
9 2015, 2015.

10 Wunch, D., Toon, G. C., Blavier, J.-F. L., Washenfelder, R. A., Notholt, J., Connor, B. J.,
11 Griffith, D. W. T., Sherlock, V., and Wennberg, P. O.: The Total Carbon Column Observing
12 Network, *Philosophical Transactions of the Royal Society of London A: Mathematical,*
13 *Physical and Engineering Sciences*, 369, 2087-2112, 10.1098/rsta.2010.0240, 2011.

14 Yokota, T., Yoshida, Y., Eguchi, N., Ota, Y., Tanaka, T., Watanabe, H., and Maksyutov, S.:
15 Global Concentrations of CO₂ and CH₄ Retrieved from GOSAT: First Preliminary Results,
16 *SOLA*, 5, 160-163, 10.2151/sola.2009-041, 2009.

17 Zander, R., Mahieu, E., Demoulin, P., Duchatelet, P., Roland, G., Servais, C., Mazière, M. D.,
18 Reimann, S., and Rinsland, C. P.: Our changing atmosphere: Evidence based on long-term
19 infrared solar observations at the Jungfraujoch since 1950, *Science of The Total Environment*,
20 391, 184-195, <http://dx.doi.org/10.1016/j.scitotenv.2007.10.018>, 2008.

21 Zellweger, C., Ammann, M., Buchmann, B., Hofer, P., Lugauer, M., Rüttimann, R., Streit, N.,
22 Weingartner, E., and Baltensperger, U.: Summertime NO_y speciation at the Jungfraujoch,
23 3580 m above sea level, Switzerland, *Journal of Geophysical Research: Atmospheres*, 105,
24 6655-6667, 10.1029/1999JD901126, 2000.

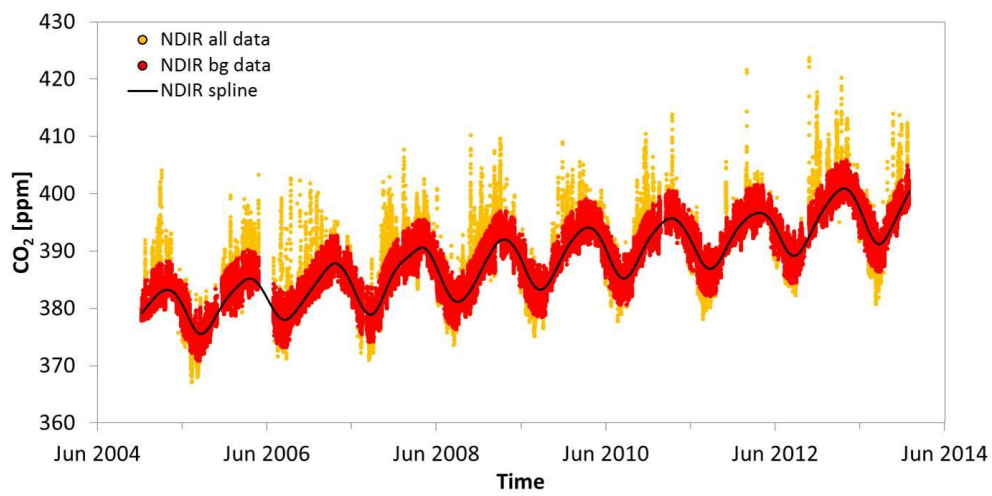
25 Zellweger, C., Forrer, J., Hofer, P., Nyeki, S., Schwarzenbach, B., Weingartner, E., Ammann,
26 M., and Baltensperger, U.: Partitioning of reactive nitrogen (NO_y) and dependence on
27 meteorological conditions in the lower free troposphere, *Atmos. Chem. Phys.*, 3, 779-796,
28 10.5194/acp-3-779-2003, 2003.

29 Zellweger, C., Hüglin, C., Klausen, J., Steinbacher, M., Vollmer, M., and Buchmann, B.:
30 Inter-comparison of four different carbon monoxide measurement techniques and evaluation

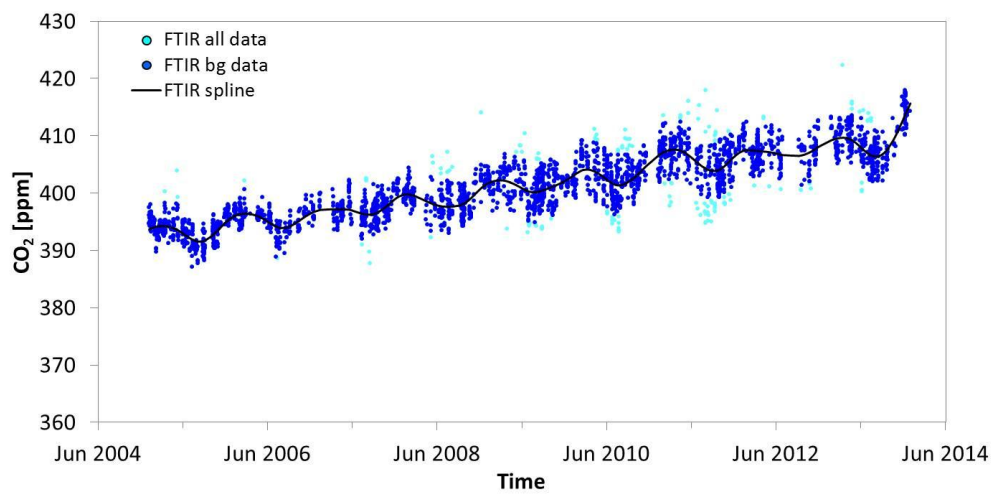
1 of the long-term carbon monoxide time series of Jungfraujoch, *Atmos. Chem. Phys.*, 9, 3491-
2 3503, 10.5194/acp-9-3491-2009, 2009.

3 Zeng, N., Zhao, F., Collatz, G. J., Kalnay, E., Salawitch, R. J., West, T. O., and Guanter, L.:
4 Agricultural Green Revolution as a driver of increasing atmospheric CO₂ seasonal amplitude,
5 *Nature*, 515, 394-397, 10.1038/nature13893, 2014.

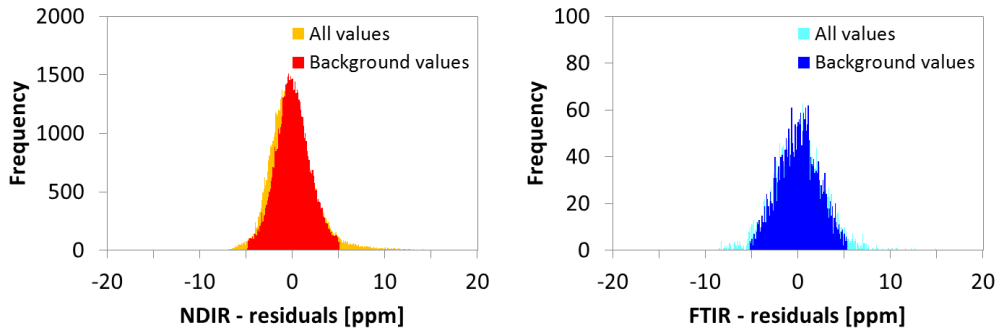
6



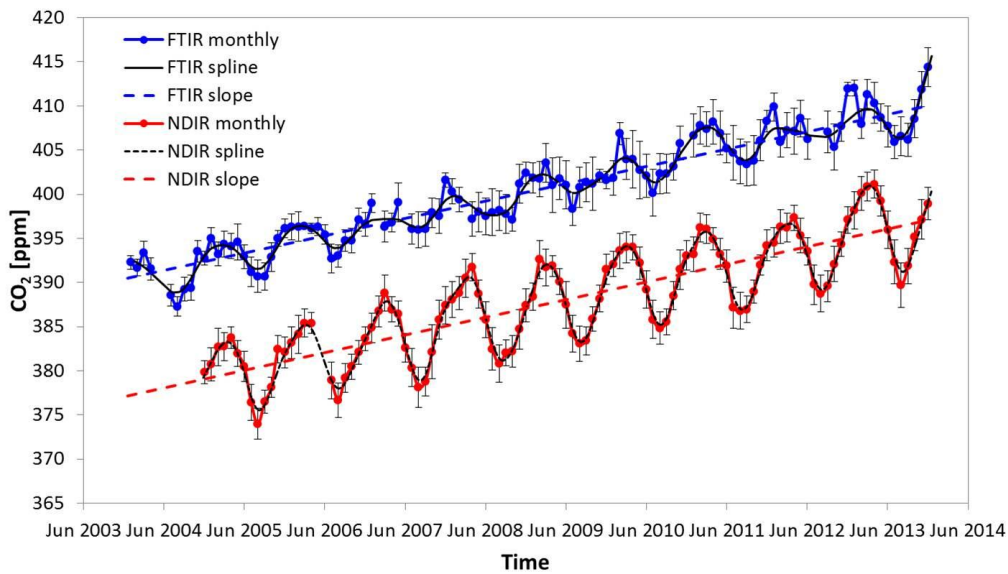
1
 2 Figure 1. In-situ CO₂ mole fractions of the NDIR measurements as a function of time in ppm
 3 at JFJ: All hourly averages before filtering (yellow), hourly averages after filtering (red) and
 4 the spline (black line). Note that the yellow points correspond to only about 5 % of the whole
 5 dataset.
 6



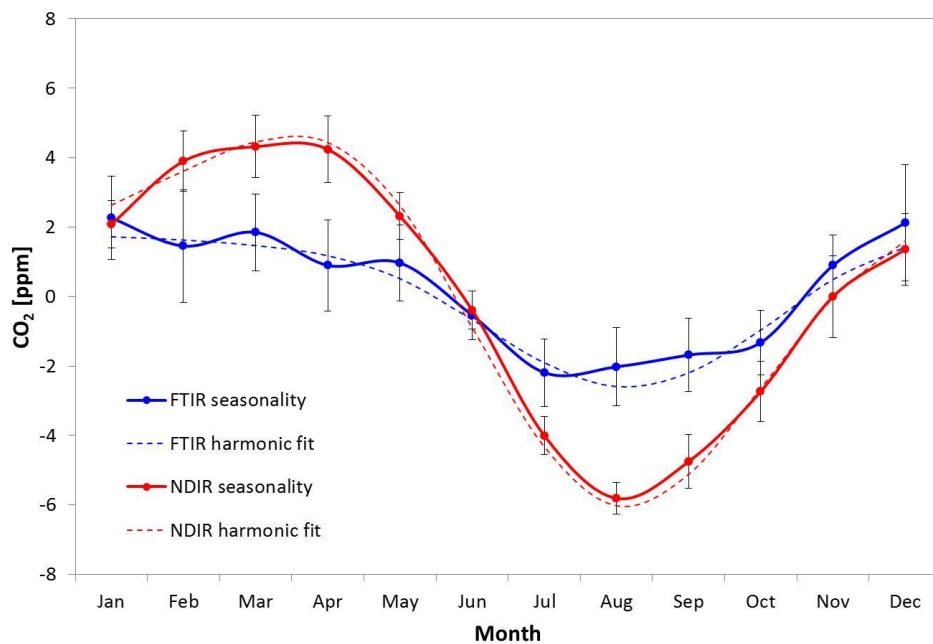
1
2 Figure 2. CO₂ mole fractions of the FTIR measurements as a function of time in ppm in the
3 column above JFJ: All hourly averages before filtering (light blue), hourly averages after
4 filtering (dark blue) and the spline (black line). The light blue points correspond to about 5 %
5 of the whole dataset.
6



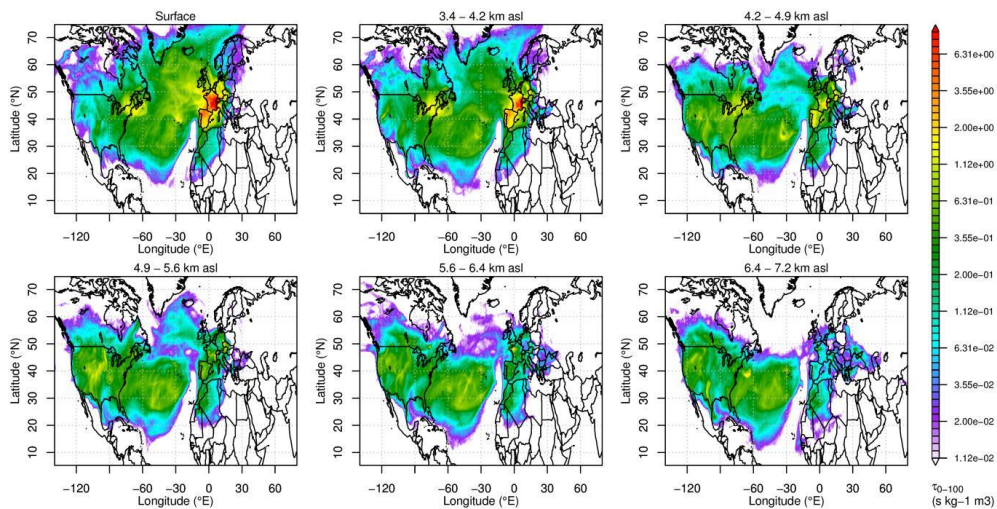
1
 2 | Figure 3. A: Histogram of all NDIR residuals (yellow) and the filtered NDIR residuals
 3 | representing the background values (red) of the in-situ measurements ~~and the rejected values~~
 4 | ~~(black)~~; B: Histogram of all FTIR residuals (light blue) and the filtered FTIR residuals
 5 | representing the background values (blue) of the column, ~~measurements and the rejected~~
 6 | ~~values (black)~~.
 7



1
 2 Figure 4. FTIR and NDIR CO₂ measurements at JFJ as a function of time: Monthly averages
 3 of the filtered FTIR data (blue), spline (black line), the annual CO₂ increase calculated from
 4 the filtered FTIR dataset (blue dashed line), monthly averages of the filtered NDIR data (red),
 5 spline (black dotted line) and the annual CO₂ increase calculated from the filtered NDIR
 6 dataset (red dashed line).
 7

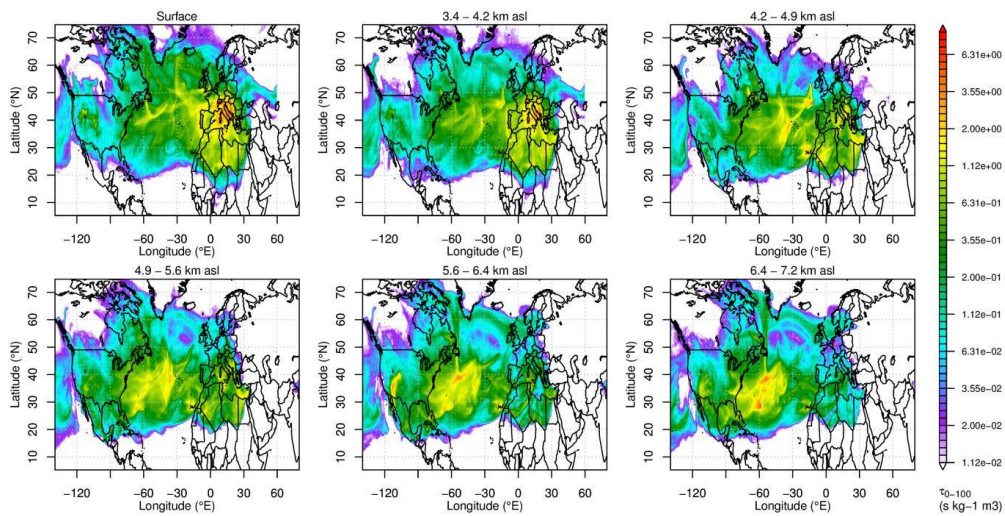


1
 2 Figure 5. Monthly averaged seasonality of the filtered FTIR and NDIR CO₂ measurements for
 3 the nine years of the comparison: averaged NDIR seasonality (red), two harmonic fit of the
 4 NDIR seasonality (red dashed line), averaged FTIR seasonality (blue) and two harmonic fit of
 5 the FTIR seasonality (dashed blue line).
 6

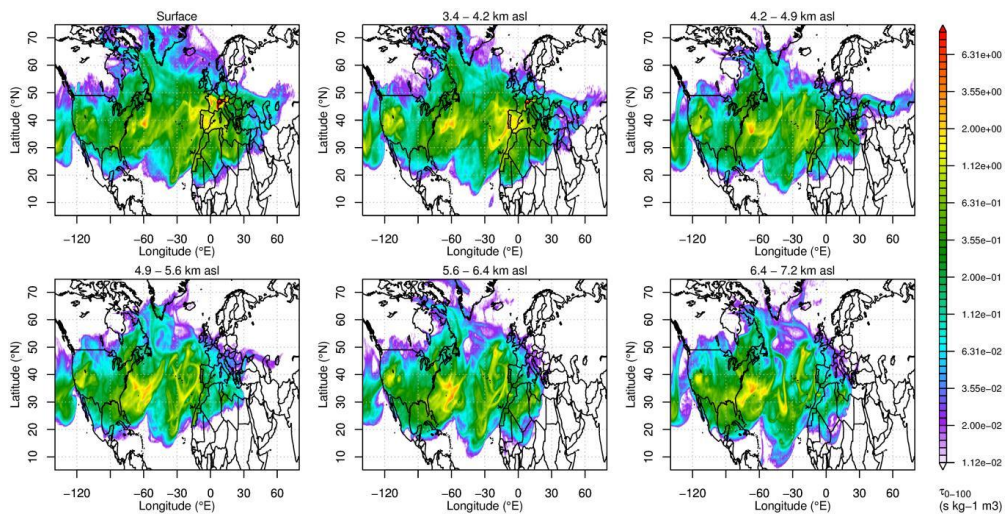


1
 2 Figure 6. Surface source sensitivity (footprints) of the air masses at JFJ (surface in-situ) and in
 3 the sub-columns above JFJ in August (CO_2 minimum of FTIR and NDIR time series) in the
 4 period 2009 to 2011 simulated with FLEXPART. The height of the sub-columns is given
 5 above the according subplots, the x-axis is the longitude, the y-axis represents the latitude, the
 6 color code of the sensitivity is given at the right side.

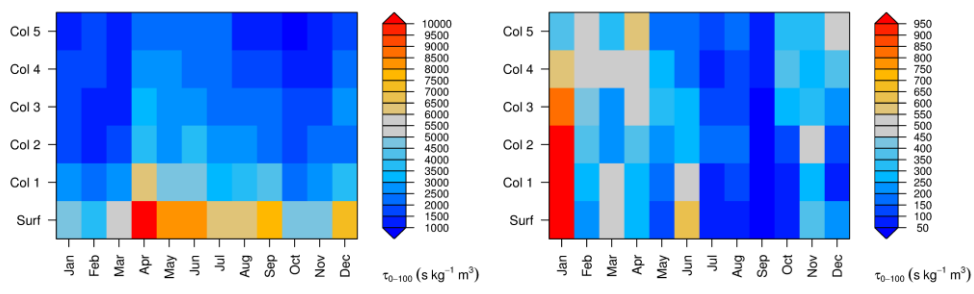
7



1
 2 Figure 7. Surface source sensitivity (footprints) of the air masses at JFJ (surface in-situ) and in
 3 the sub-columns above JFJ in January (CO_2 maximum of the FTIR dataset) in the period 2009
 4 to 2011 simulated with FLEXPART. The height of the sub-columns is given above the
 5 according subplots, the x-axis is the longitude, the y-axis represents the latitude, the color
 6 code of the sensitivity is given at the right side.
 7

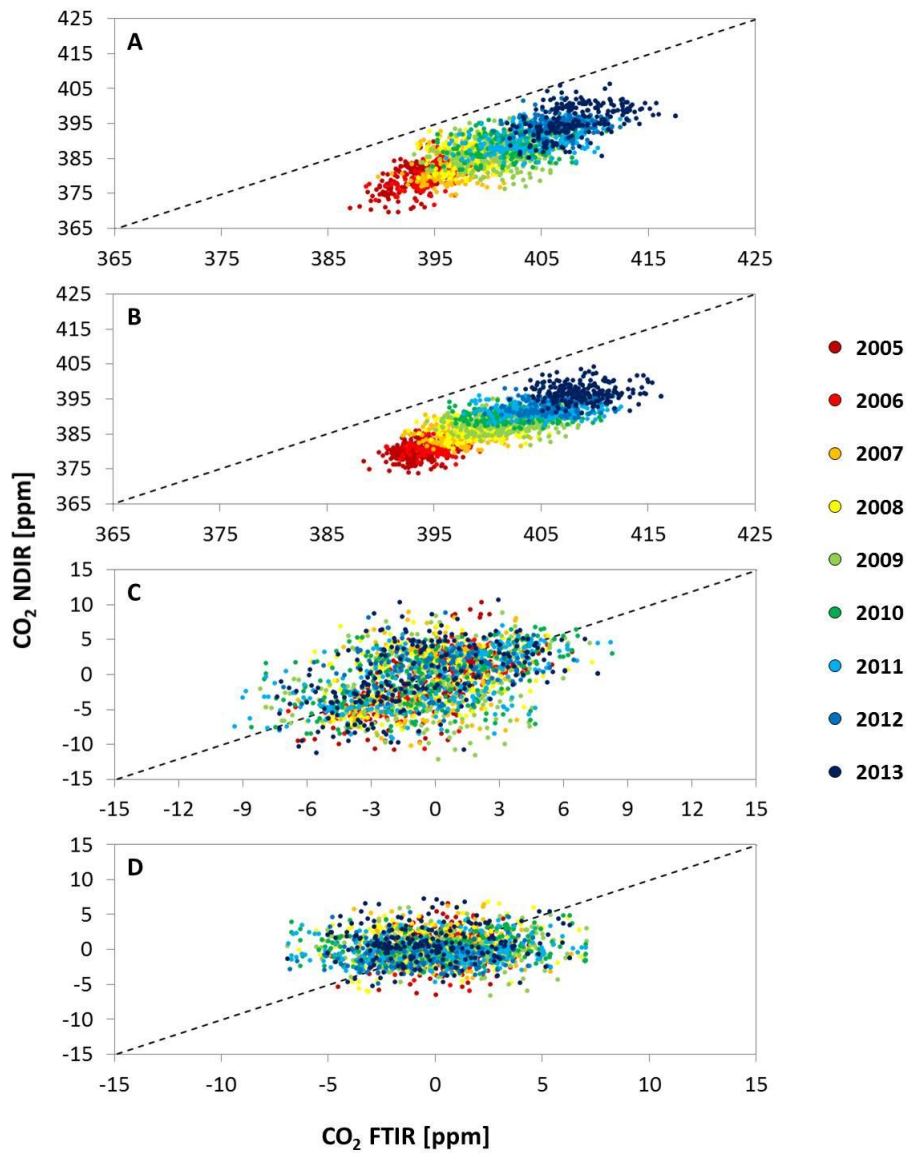


1
 2 Figure 8. Surface source sensitivity (footprints) of the air masses at JFJ (surface in-situ) and in
 3 the sub-columns above JFJ in March (CO₂ maximum of the NDIR dataset) in the period 2009
 4 to 2011 simulated with FLEXPART. The height of the sub-columns is given above the
 5 according subplots, the x-axis is the longitude, the y-axis represents the latitude, the color
 6 code of the sensitivity is given at the right side.
 7

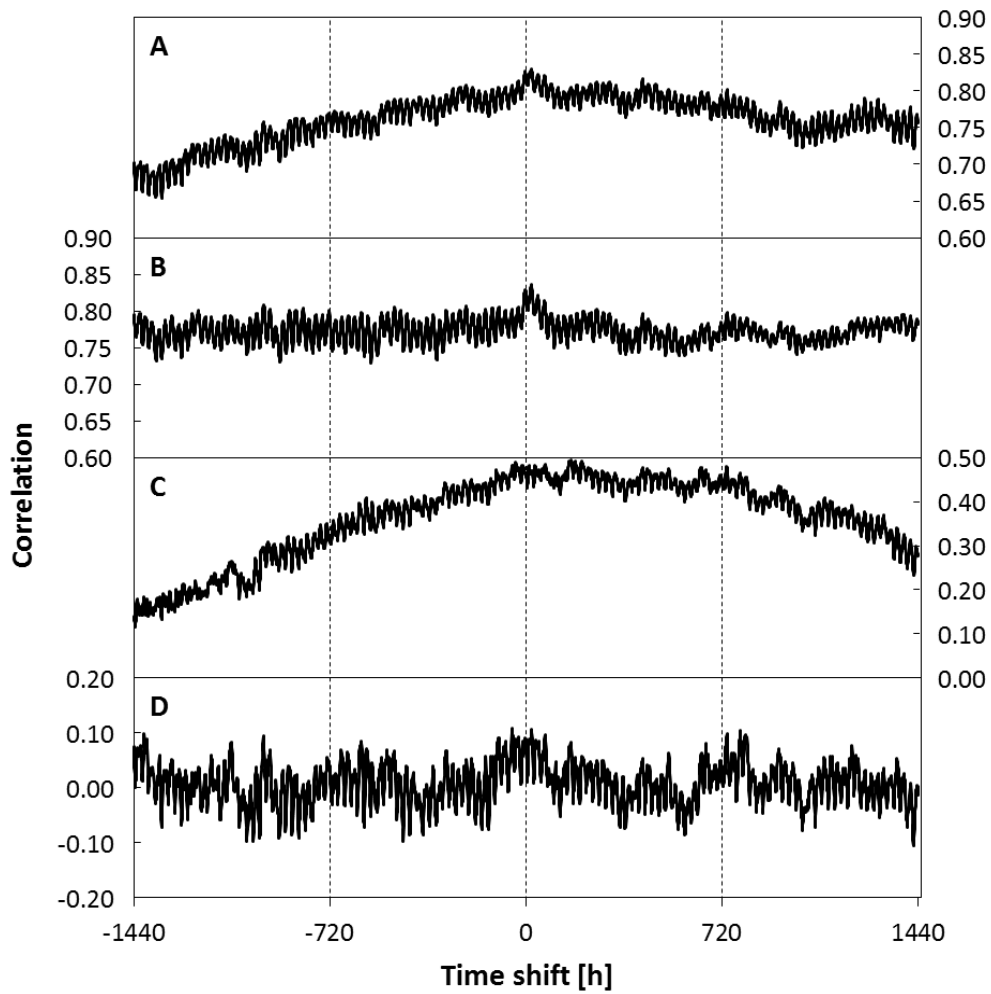


1
 2 Figure 9. Annual cycle of FLEXPART derived total surface residence time over land for
 3 different vertical arrival columns above Jungfraujoch: (left) for land surfaces north of 30°N
 4 and (right) for land surfaces south of 30°N.

Formatted: English (U.S.)
 Field Code Changed
 Formatted: English (U.S.)

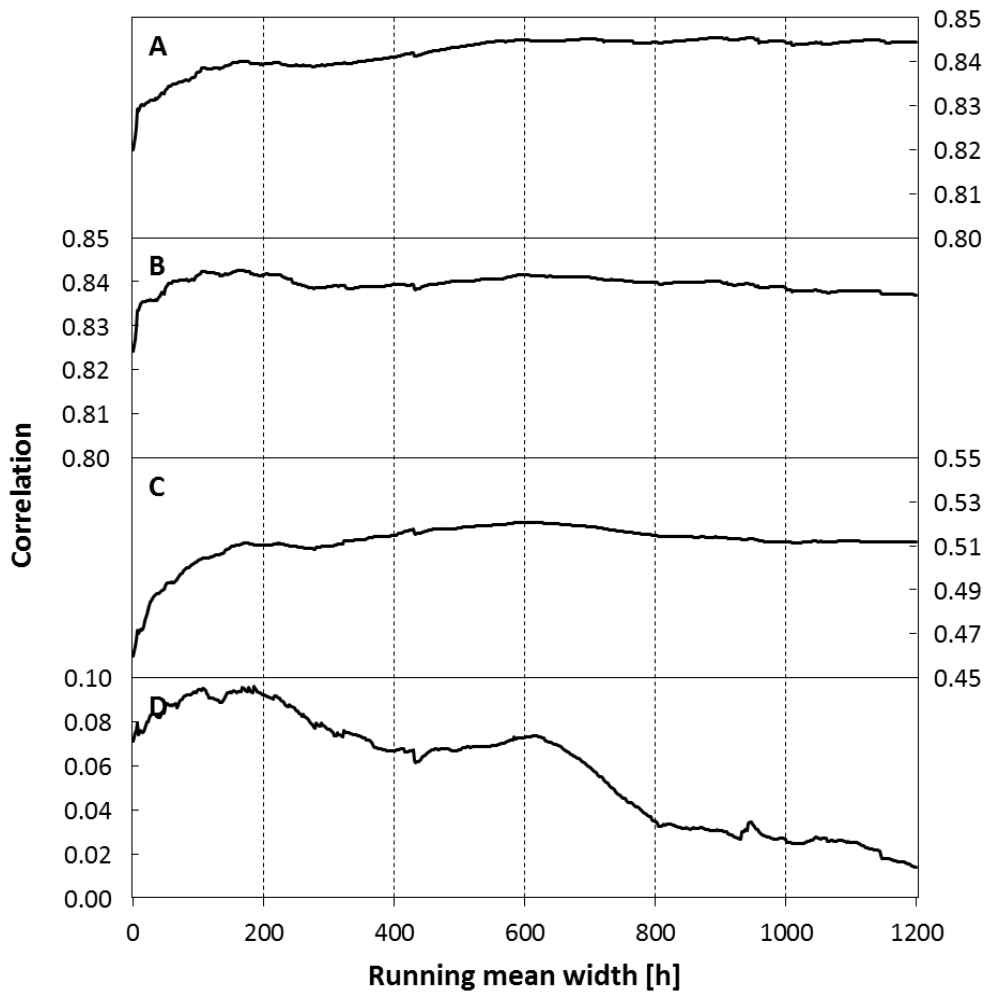


1
2 Figure 10. Correlation plots of the filtered hourly NDIR CO₂ measurements vs. the filtered
3 FTIR CO₂ measurements. The different colors refer to the years 2005 to 2013 (see legend). A:
4 The NDIR CO₂ measurements vs. FTIR CO₂ measurements including both, the annual CO₂
5 increase and the seasonality; B: As A but without seasonality; C: As A but detrended; D: As
6 A but with neither annual CO₂ increase nor seasonality. The dashed line is the 1:1 line.
7



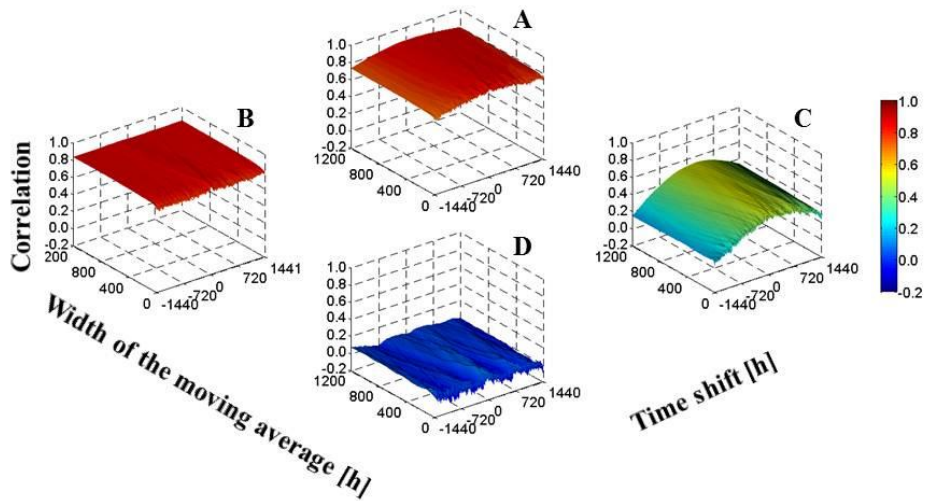
1
 2 Figure 11. Evolution of the correlation between the filtered FTIR and NDIR datasets with
 3 changing time shift. A: Correlation between complete datasets; B: Correlation between the
 4 two datasets without seasonality; C: Correlation between the two datasets without trend; D:
 5 Correlation between the two datasets with neither trend nor seasonality.

6



1
 2 Figure 12. Change of the correlation between the filtered FTIR and NDIR datasets with
 3 increasing width of the running mean. A: Correlation between the two datasets with
 4 seasonality and slope; B: Correlation between the two datasets without seasonality; C:
 5 Correlation between the two datasets without slope; D: Correlation between the two datasets
 6 with neither slope nor seasonality.

7



1
 2 Figure 13. Surface plots of the correlation of the NDIR CO₂ measurements vs. the FTIR CO₂
 3 measurements. The x-axis corresponds to the time shift, the y-axis to the width of the moving
 4 average and the z-axis to the correlation between the FTIR and the NDIR dataset, the color
 5 code illustrates the correlation and corresponds to the z-axis values. A: The FTIR CO₂
 6 measurements vs. the corresponding NDIR CO₂ measurements including the annual CO₂
 7 increase as well as the seasonality; B: As A but without seasonality; C: As A but detrended;
 8 D: As A but detrended and deseasonalized.